COVER SHEET

Study of Viscoelastic and Friction Damper Configurations in Medium-Rise Structures

Julius Marko, David Thambiratnam and Nimal Perera*
School of Urban Development
Queensland University of Technology
Brisbane, Queensland, Australia
*Bird & Marshal Ltd., London, UK

Abstract

This paper presents a comprehensive study on the seismic mitigation of medium rise frame-shear wall structures using embedded dampers. Two building structures with embedded viscoelastic and friction dampers in different configurations and placed in various locations throughout the structure are subjected to five different earthquake loadings. Finite element techniques are used to model the dampers and the structures and to obtain the dynamic responses. Influence of damper type and properties, configuration and location are investigated using time history responses. Results for tip deflection and acceleration are evaluated for a number of cases and demonstrate the feasibility of the technique for seismic mitigation of these structures for a range of excitations, even when the dominant seismic frequencies match the natural frequency of the structure. Results also provide information which can be used for optimal damper placement for seismic mitigation.

1. Introduction

Under earthquake activity buildings have known to suffer extensive damage and even total collapse. In order to achieve satisfactory earthquake response of a structure, three methods can be identified as being practical and efficient. These are; *structural isolation*, energy absorption at *plastic hinges* and use of *mechanical devices* to provide structural control.

In recent times there has been interest in the use of mechanical energy absorbing devices located within the structure. These mechanical energy absorbers have been found to be quite promising and they form the focus of the present study. These devices absorb the energy from the earthquake, reducing the effects on the critical components of the structure. After the earthquake, these absorbers, which do not themselves support the normal loads of the structure, can be replaced leaving the building undamaged.

There are two types of structural control provided by the addition of mechanical devices; active and passive control. *Active control* requires a power supply to activate the dampers and hence may be undependable during seismic events where the power supply could be disrupted. For this reason, dampers with active control have been tested on tall buildings subjected to wind induced loading rather than the more unpredictable cyclic loading caused by earthquakes.

On the other hand, *passive energy dissipation systems* have emerged as special devices that are incorporated within the structure to absorb a portion of the input seismic energy. As a result, the energy dissipation demand on primary structural members is often considerably reduced, along with the potential for structural damage.

The idea of utilizing separate *passive energy dissipating dampers* within a structure to absorb a large portion of the seismic energy began with the conceptual and experimental work of Kelly et al. (1972). Today there are various types of manufactured passive dampers available in the market which use a variety of materials to obtain different levels of stiffness and damping. These dampers have been reviewed by Constantinou et al. (1998), and Sadek et al. (1996). Some of these include viscoelastic,

viscous fluid, friction and metallic yield dampers. These dampers have different dynamic characteristics and so will affect the seismic response of structures differently.

The characteristics of *viscoelastic (VE)* and *viscous dampers* are that, they dissipate energy at all levels of deformation and over a broad range of excitation frequencies. *Friction dampers* on the other hand, dissipate energy only when the slip force is reached and exceeded. A combination of these dampers can be used within the structural system to effectively damp out the high and low frequency contents of earthquakes (Hisano at al. 2000; Shao at al. 1999). This is commonly referred to as a *hybrid system*.

There have been several studies undertaken to develop a method which optimises the use of energy dissipating dampers in vibration control of buildings under earthquake loads (Abdullah et al.1993; Aiken et al. 1990; Ashour et al.1987; Constantinou et al. 1983; Hahn et al. 1992; Hanson 1993; Hanson et al. 1993; Madsen 2001; Natke 1993; Ray et al. 1974; Ribakov et al. 1999 and Zhang et al. 1992). However the basic theories behind these methods are mostly not supporting each other and in many ways are rather contradicting. Even more, there are numerous types of dampers available commercially as well as numerous types of high-rise buildings which could be treated under seismic loads with varied properties. This could produce a wide range of results as will be discussed later in this paper. In the light of this, there is still a great necessity for further development of methods to determine the optimal use of dampers in high rise buildings.

This comprehensive study investigated the mitigation of the seismic response of 18-storey and 12-storey frame-shear wall structures with embedded dampers. Three damping mechanisms were used, viz, (i) displacement-dependant friction dampers, (ii) velocity-dependant VE dampers and (iii) hybrid system which is a combination of friction and VE dampers. Six different damping systems, arising from these three damping mechanisms in different configurations were studied. These were, friction and VE diagonal dampers, friction and VE chevron brace dampers, hybrid friction-VE dampers and VE lower toggle dampers. The damping systems were embedded in six different locations (one at a time) within cut-outs of the shear wall in the structure. Damper properties such as stiffness, damping coefficient, location, configuration and size were varied to obtain tip deflections and accelerations from time history analyses under five different earthquake records.

The results of this study will provide information for optimising the use of embedded dampers in seismic mitigation of medium-rise building structures.

2. Model description

2.1 Damper Properties

Finite Element (FE) methods have been employed to model, analyse and investigate the effects of these three types of damping devices and their configurations on the seismic response of the structures. The program selected for the numerical analysis in this study was ABAQUS/Standard Version 6.3. In conjunction with this program, MSC/PATRAN 2003 has been used as the pre-processor for generating the geometry, element mesh, boundary conditions and loading conditions of the model, and as the post-processor for viewing the results of the analysis.

A direct integration dynamic analysis was selected to obtain the response of the structure under seismic loading. This analysis assembles the mass, stiffness and damping matrices and solves the equations of dynamic equilibrium at each point in time. The response of the structure is obtained for selected time steps of the input earthquake accelerogram. The dynamic procedure in ABAQUS/Standard uses implicit time integration. To study the effectiveness of the damping system in mitigating the seismic response of the buildings in this study, the maximum displacements and accelerations at the tip of the structure are obtained from the results of the analysis and compared with those of the undamped building structure.

The first damping mechanisms used in this study were represented by *friction dampers*. The initial focus of this research was on the development of a model which represents the real behaviour of friction dampers. This was achieved by modelling the frictional contact between two tubes with one sliding inside the other.

The extended version of the classical isotropic Coulomb friction model is provided in the computer program ABAQUS, (the program available to the authors) for use with all contact analyses. In the basic form of the Coulomb friction model, two contacting surfaces can carry shear stresses up to certain magnitude across their interface before they start sliding relative to one another.

In two-dimensional contact problems, the direction of frictional slip must lie in the plane, and hence, there are only two options: slip to the right or left. The contact problem is therefore in the linear range, since all the states are governed by linear equations and nonlinearity is introduced only through the inequalities that trigger changes of state.

The second damping mechanisms used in this study was represented by *VE dampers*. A VE damper was modelled as a linear spring and dash-pot in parallel (known as the Kelvin model) where the spring represents stiffness and the dashpot represents damping. Abbas et al. (1993) define the stiffness and damping coefficients as follows:

$$k_d = \frac{G'A}{t} \tag{1}$$

$$C_d = \frac{G''A}{ft} \tag{2}$$

where, A is the shear area of the VE material, t is the thickness of the VE material f is the loading frequency of the VE damper, G' is the shear storage modulus, G'' is the shear loss modulus and T is temperature in ^{0}C. The following expressions were used to obtain the moduli of the VE material as defined by Abbas et al.(1993):

$$G' = 16.0\, f^{0.51} \gamma^{-0.23} e^{(72.46/T)} \tag{3}$$

$$G'' = 18.5\, f^{0.51} \gamma^{-0.20} e^{(73.89/T)} \tag{4}$$

where γ is the shear strain. Temperature variations will have an effect on damper properties as evident from equations (3) and (4), and hence on the results. We have not considered temperature effects in this paper. This model approximates the true behaviour of a VE damper under vibratory loading to within 10%, which was considered sufficiently accurate for the purposes of this study. In order to create a computer model, appropriate values of the frequency of loading applied to the damper, the shear strain and the temperature of the VE material have to be selected. In this investigation, the ambient temperature of the VE material was assumed to be 21 ^{0}C, the shear strain, γ, was assumed to remain constant at 100%. This was done as it has been shown that a large decrease in the stiffness occurs in the 0-50% strain range, whereas in the 50-200% strain range the stiffness remains approximately constant. For the loading frequency, f, the first mode of vibration of the structures was used because it was assumed that the structure will predominantly vibrate in this mode.

The third damping mechanisms used in this study was represented by a *hybrid friction-VE damper* consisting of a combination of VE and friction damper model in series.

Different configurations consisting of diagonal, chevron brace, hybrid diagonal-chevron brace and lower toggle configuration of each of these damping mechanisms at different location in the structure were considered to investigate their influence on seismic mitigation.

2.2. Description of structure – damper models

The structural models, treated in this paper have been represented by two types of frame-shear wall structures. The first set of models represents two-dimensional medium-rise 18-storey structures. The shear walls of these models were constructed using shell elements of designation S4R5, having 4 nodes per element and five degrees of freedom at each node. The dimensions of the shear walls were 6m wide and 0.4 m thick. The columns and beams were located on either side of the wall, as seen in Fig. 1. The column and beams had cross-sectional dimensions of 0.75 x 0.75 m and 0.75 x 0.45 m

respectively and the beam spans were 6.0 m. The height between storeys was set at 4.0 m, which made the overall height of the structures to be 72.0 m.

The second set of models (Fig. 2.) represents 12-storey structures each with a shear wall of the same parameters as was used in the previous models and columns and beams had cross-sectional dimensions of 0.6 x 0.6 m and 0.6 x 0.45 m respectively. The spans of the beams were 6.0 m and the height between storeys was 4.0 m, which made the overall height 48.0 m.

The natural frequency of the 18-storey undamped structure was 0.614 Hz and in the range 0.570 - 0.650 Hz when fitted with dampers, while the natural frequency of the 12-storey undamped structure was 1.050 Hz and in range 0.951 - 1.100 Hz when fitted with dampers. These values are within the range of dominant frequencies of all the earthquakes chosen in this investigation (varying from 0.58 Hz to 1.07 Hz, as will be seen later) and hence this study treats the structural response under a range of seismic excitations including a resonant range.

A total of six different damping systems were considered. Seismic analyses were carried out with one type of damping system at a time. Four different configurations of the VE and friction dampers were considered- diagonal, chevron brace, lower toggle and a hybrid configuration with the friction damper oriented horizontally and the VE damper mounted diagonally. Furthermore, six different damper placements as shown in Figs. 1 and 2 were used in each structural model to study the influence of location on their seismic response. The undamped structures were also analysed in order to compare results.

Concrete material properties were chosen since many high-rise buildings are constructed by using reinforced concrete. The concrete had a compressive strength, f'_c of 32 MPa, Young's modulus, E_c of 30,000 MPa, which assumes predominantly elastic response with little wall cracking, Poisson's ratio, υ of 0.2, and density, ρ of 2500 kg/m^3. No internal damping for the concrete was taken into consideration as it was assumed to be small in relation to the damping added by the devices. Structural steel was used to model friction dampers and hybrid dampers with Poisson's ratio υ of 0.3 and density, ρ of 7700 kg/m^3. The coefficient of friction was 0.25 for the friction dampers.

2.2.1. Models with friction dampers – diagonal configuration

After preliminary convergence study, the concrete shear walls were modelled with 2016 S4R5 shell elements for 18-storey and 1344 S4R5 shell elements for 12-storey structures respectively.

Details of the damper located within shear wall of the frame-shear wall model can be seen in Fig. 3, where a 3.5 m wide by 3.5 m high wall section has been cut out and replaced by a diagonal friction damper. In creating a frictional damper, there were a few options in the computer program Abaqus, available to the authors. The best results were achieved with the particular model described below. The validity of results, however, is restricted to the nominal damper properties assumed.

The damper was modelled as a pair of diagonal tubes each with a thickness of 50 mm, and with one tube placed within the other.

- The outer tube having an inner diameter of 200 mm and length 3.75 m was modelled using 264 S4R5 shell elements.
- The inner tube having an outer diameter of 198 mm and length 3.75 m was modelled using 252 S4R5 shell elements.

The radial clearance between the tubes was 1mm and the contact area in the unloaded state was 3.71 m^2. The connection between each tube and the shear wall was modelled using a MPC (Multi-Point Constraint) Pin type connecting element, which provides a pinned joint between two nodes. This MPC makes the displacement of the two nodes equal but allows differential rotations, if these exist, independent of each other. A MPC Slider type connecting element was chosen to ensure frictional sliding between the tubes in a determined direction. This MPC keeps a node on a straight line defined by two other nodes such that the node can move along the line, and the line can also change length. Fig. 3 also shows the details of the MPC connection between the damper and shear wall in the computer model. The efficiency of these dampers as well as that of the other damping systems described below, were analysed under the five earthquake excitations.

2.2.2. Models with VE dampers – diagonal configuration

The concrete frame-shear wall structure was modelled using the same FE mesh, material properties and dimensions as described above. Details of the diagonal VE damper located within the cut out of the shear wall can be seen in Fig. 4. The properties of the damper for 18-storeys models were first calculated as k_d = 10 x 10^6 N/m and C_d = 63x10^6 Ns/m based on double layer damper in parallel with dimensions of 1,850 mm by 300 mm by 10 mm and the values G' = 900,000 Pa and G" = 350,000 Pa. These moduli were calculated using the loading frequency f = 0.614 Hz, which corresponded to the fundamental frequency of this structure model. In a similar manner, damping properties of VE dampers located in the 12-storeys models (with f = 1.05 Hz), were calculated. The values for this structure had k_d = 10 x 10^6 N/m and C_d = 38 x 10^6 Ns/m with dimensions of 1,670 mm by 300 mm by 10 mm and the values G' = 950,000 Pa and G" = 450,000 Pa.. The results for both structure were evaluated and in order to facilitate comparisons, approximate average values of k_d = 10 x 10^6 N/m and C_d = 50 x 10^6 Ns/m, were used in all the subsequent analyses.

2.2.3. Models with hybrid friction-VE dampers

The hybrid friction-VE damper was created to represent 50% of the damping force of the diagonal VE damper, and 66.6% of the damping force of the chevron brace friction dampers. It was anticipated that results for structures fitted with a hybrid friction-VE damper which contains the displacement dependant friction part, and the velocity dependant VE part, can provide more effective control of the structure response.

The concrete frame-shear wall structures were using the FE mesh, material properties and dimensions as before. The only difference was in the size of the cut out which was reduced to 3.5 m wide by 2.5 m high.

The friction component of the hybrid friction-VE damper was modelled as a pair of horizontal tubes, with one tube placed within the other.

- The outer tube was constructed from 384 S4R5 shell elements, the inner diameter of this tube was 200 mm and its length was 1.500 m.
- The inner tube was constructed from 155 S4R5 shell elements, the outer diameter of this tube was 396 mm and its length was 1.4850 m.

The thickness of both tubes was 50 mm, the radial clearance between the tubes was 1 mm, the contact area in the unloaded state was 1.67 m^2 and the coefficient of friction between the tubes was 0.25. The direction of frictional sliding was determined by Slider and Pin type MPCs.

The VE part of the hybrid damper which represented both spring and dashpot elements was oriented with one end attached to a steel holder placed in the middle of the upper edge of the cut out, and the other end attached to the lower left-hand corner of the cut out, as shown in Fig. 5. This oriented the damper at 45^0 to the horizontal while its length was 2.475 m. The values of damping and stiffness were kept the same as in the model with diagonal VE dampers.

The hybrid damper is expected to utilise the desirable features of both the VE and friction components. But, these dampers combining VE and friction components in series can cause a practical problem, if the 2 components are not properly isolated. As the VE material dissipates energy it heats and softens, while the frictional element does not and hence at a certain point the frictional element will not be pushed hard enough to slip

2.2.4. Models with friction dampers – chevron brace configuration

The concrete frame-shear wall model was created using the same FE mesh, material properties and dimensions as the model incorporating hybrid dampers. Fig. 6 shows the detail of frame-shear wall model with a friction damper of chevron brace configuration. The friction damper is modelled as a pair of horizontal tubes, where one tube is placed within the other.

- The outer tube was constructed from 264 S4R5 shell elements, the inner diameter of this tube was 200 mm and its length was 2.565 m.
- The inner tube was constructed from 276 S4R5 shell elements, the outer diameter of this tube was 276 mm and its length was 2.565 m.

The thickness of both tubes was 50 mm, the radial clearance between the tubes was 1 mm, and the contact area in the unloaded state was 3.09 m^2. The connection between each tube and the shear wall

was modelled using a MPC Pin type connecting element, and a MPC Slider type connecting element was chosen to ensure frictional sliding between the tubes in a determined direction. The details of the MPC connection between the damper and shear wall in the computer model are also shown in Fig.6.

2.2.5. Models with VE dampers – chevron brace configuration

The concrete frame-shear wall model was created as in the previous case. The damper placed within the shear wall, as shown in Fig. 7, was oriented horizontally in the upper part of the cut out, attached at one end directly to the left side of the shear wall and attached at the other end to the upper edge of the shear wall via an MPC Rigid connection.

2.2.6. Models with VE dampers – lower toggle configuration

Quite recently several new configurations of passive energy dissipation devices have emerged Constantinou et al.(2000). These configurations utilize innovative mechanisms to amplify displacement and hence lower input force demand in the energy dissipating devices. They have, however, not received attention comparable to the more traditional diagonal and chevron brace configurations, probably due to their complex nature. These new configurations include the upper, lower and reverse toggle systems. One of them, the lower toggle system was considered in this study.

The concrete frame-shear wall models were created using the FE mesh, material properties and dimensions as before. The only difference was in the size of the cut out which was enlarged to 3.5 m wide by 3.0 m high. Detail of the lower toggle VE damper located within the cut out of the frame-shear wall model can be seen in Fig. 8. This damper oriented at 45^0 to the horizontal with its length of 2.262 m had one end attached to the lower arm of the steel holder and the other end attached to the lower right-hand corner of the cut out. In this configuration, the arms of the brace assembly were created from 100 x 5 SHS and these arms were connected to each other by 6mm pre-bent plate and the connection to the shear wall was by MPC Pin.

These structural models have natural frequencies which match those of typical medium rise buildings and hence the results could have wider application.

3. Earthquake records

In general, all earthquake records possess different properties such as peak acceleration, duration of strong motion and ranges of dominant frequencies and therefore have different influences on the structure. In order to ensure that the chosen mitigation procedure is effective under different types of excitations, five, well-known earthquakes records were used in this study. These were all applied for the first 20s of their duration. For more consistent comparison, all earthquake records were scaled to a peak acceleration of 0.15 g. Duration of the strong motion and range of dominant frequencies were kept unchanged and were evaluated by Welch's method (1967), based on Fast Fourier Transform Techniques, using the computer program MATLAB Version 6.5. The earthquake records which have been selected to investigate the dynamic response of the models are:

- El Centro (1940) with strong motion during 1.5-5.5 secs and dominant frequencies in the range 0.39-6.39 Hz,
- Hachinohe (1994) with strong motion during 3.5-7.5 secs and dominant frequencies in the range 0.19-2.19 Hz,
- Kobe (1995) with strong motion during 7.5-12.5 secs and dominant frequencies in the range 0.29-1.12 Hz,
- Northridge (1994) with strong motion during 3.5-8.0 secs and dominant frequencies in the range 0.14-1.07 Hz and
- San Fernando (1971) with strong motion during 4.5-9.5 secs and dominant frequencies in the range 0.58-4.39 Hz.

Graphs of these earthquake records and their dominant frequencies are for convenience presented in Fig. 9-13.

4. Results and Discussion

4.1. 18-storey models

The first type of the medium rise structure which was investigated in this paper was represented by the 18-storey frame-shear wall model described in section 2.2. The results for this structure under five earthquake excitations are presented below.

There are various ways of assessing seismic response, but computation of tip deflection is a reasonable measure of the overall effect of the earthquake. Working back from tip deflection to equivalent base shear and moment is one way of 'averaging out' the seismic effects of varying accelerations up the wall. Hence any reduction in tip deflection represents a worthwhile reduction in overall seismic design force. The results presented below show that this reduction is dependent on the complex characteristics of the time histories used for assessment and hence the benefits can only be legitimately assessed if the analysis is carried out for the suite of time histories.

Figs.14-18 illustrates the typical time history responses of the structure of designation H1-3 with the diagonal friction and VE dampers fitted in the lowest three storeys. These graphs illustrate tip deflection and tip acceleration responses under five earthquake excitations compared with the responses of the undamped structure. From these graphs it is evident that the dampers embedded into the cut-outs of shear walls significantly reduced the tip deflection and acceleration throughout the duration of the earthquakes. However from these graphs, as well as from numerous other results obtained with dampers at different placements, it was also evident that the different damping properties of the friction and VE dampers resulted in different responses. The friction dampers in the vast majority of cases surpassed the VE dampers in their ability to reduce the intensity of the initial strong motion. In contrast, the advantage of the VE dampers was in gradually decreasing the tip deflection and tip acceleration of the structure.

4.1.1. Undamped structural model

The undamped structural model was created in order to compare its results with the results of the structures fitted with the damping systems. The results of the tip deflection and tip acceleration of this structure experienced under five earthquake excitations are presented in Table 1.

4.1.2. Structural models with friction and VE dampers – diagonal configuration

Table 2 illustrates the results of the percentage reductions in the peak values of the tip deflection experienced by the structures fitted with the diagonal friction dampers. It is evident that the dampers display a wide range of efficiency, with significant reductions in most cases with an average reduction of 23.6% under the Hachinohe earthquake. In some cases, there are increases, especially under the San Fernando earthquake. This may be attributed to inadequate compensation for removed stiffness and/or partial resonance of the damped structure and insufficient push on the friction damper to make it fully operational.

In terms of damper placement, the highest average tip deflection reduction was achieved by the structure with dampers fitted in the top storeys, while the lowest average reduction occurred for the structures with dampers placed in the storeys 10 to 12. The results achieved under the El Centro, Hachinohe and Northridge earthquakes fully support Hanson's theory (1993), which recommends placement of friction dampers at levels of maximum interstorey drift (Table 3). On the other hand, with the Kobe and San Fernando earthquakes, a high efficiency was displayed only with dampers fitted in the lowest storeys.

Table 4 presents the percentage reduction in tip deflection of the structures embedded with the diagonal VE dampers. The overall performance of the models was significantly high; however the range of results remained wide. The average tip deflection reductions varied from 4.1% under the San Fernando earthquake, to 19.3% under the El Centro earthquake.

The best performance was achieved when the dampers were placed in the lowest storeys, while moving them towards the top of the structure resulted in a gradual decrease in tip deflection under all earthquake excitations. According to a study conducted by Ashour (1987), the optimal placement of dampers should be the one that maximises the damping ratio of the fundamental mode, as this mode's

contribution to the structure's overall response is always significant. The results revealed that the best performance was achieved when dampers were placed in the lowest parts of each structure, while placing dampers towards the top of the structure decreased the damper efficiency. These results are in accordance with Ashour's study.

Though tip deflection is more important in assessing overall seismic response, this study also investigated the reductions in the peak values of tip accelerations at the top of the structures.

Table 5 shows the tip acceleration reductions of the structures fitted with the diagonal friction dampers, compared with results of the undamped structure. In terms of efficiency of these dampers under a variety of earthquake loadings, a similar trend as per the tip deflection can be observed. The range of the results was once again very wide, varying from 16.7%, an average increase that occurred under the San Fernando earthquake, to 18.2%, an average reduction obtained under the Hachinohe earthquake.

The diagonal friction dampers achieved the highest acceleration reductions when placed in the lowest 6 storeys and in each of the storeys 13 to 15. On the other hand, when they were placed in the highest storeys a significant increase in tip acceleration was experienced. This tip acceleration increase was mainly due to the operating principle of the friction dampers, which caused transfer of acceleration to the ambient structural elements as well as decrease in stiffness of the top storeys due to the cut-out in the shear wall.

The percentage reductions in the tip acceleration at the top of the structures for the structure embedded with the diagonal VE dampers are presented in Table 6. The highest average acceleration reduction of 22.4% was obtained for the Hachinohe earthquake. However, the acceleration reductions occurred under the other earthquakes were also adequately high. The greatest tip acceleration reductions were obtained when the dampers were placed in the lowest storeys. The tip acceleration reductions were still relatively high for dampers placed in the middle storeys. On the other hand, when the dampers were placed in the top storeys an increase in tip acceleration was experienced.

4.1.3. Structural models with friction and VE dampers – chevron brace configuration

The percentage reductions in tip deflection experienced by structures fitted with the chevron brace friction dampers are illustrated in Table 7.

The performances of the dampers were within a very narrow range from 7.0%, under the Hachinohe earthquake, to 9.7%, under the Northridge earthquake respectively. In terms of the damper placement, two major trends can be observed. The first trend implies that under the Kobe and San Fernando earthquakes the highest efficiency occurred when the dampers were placed in the lowest storeys and decreased rapidly as the dampers were moved toward the top of the structures. The second trend, observed under the El Centro, Hachinohe and Northridge earthquake excitations, supports the theory that damper efficiency is increased when they are moved to the regions with large inter-storey drift.

The percentage reductions in tip deflection achieved by the structures fitted with chevron brace VE dampers are presented in Table 8. The performance of dampers under the El Centro, Hachinohe, Kobe and Northridge earthquakes were suitably consistent, whereas their performance under the San Fernando earthquake was adequate only in the lower storeys. Regarding damper placement, these dampers followed the trends similar to those of the chevron brace friction dampers.

The results of percentage reductions in tip acceleration experienced by the structures fitted with the chevron brace friction dampers are shown in Table 9. These results showed significant acceleration reductions of the structure under the El Centro, Hachinohe and Kobe earthquake, while the reductions occurred under the Northridge and San Fernando earthquakes were mostly insufficient. The highest average acceleration reduction was achieved by the dampers placed in the storeys 4 to 6. The acceleration reductions of the dampers fitted in the other storeys were considerably lower and also rather inconsistent.

Table 10 shows the reduction in tip acceleration for the chevron brace VE dampers. The highest average reduction of 10.9% was obtained under the El Centro earthquake. The results from the other excitations were obviously less significant. The highest acceleration reduction was achieved when dampers were placed in the lowest storeys, with a decrease in their efficiency as they were moved toward the top of the structures.

Both types of chevron brace dampers were created to represent only 66.6% of the damping force of the diagonal dampers. Despite this fact, the overall reductions in tip deflection were equally high

compared to those of the diagonal dampers. The reductions in tip displacement for both types of the chevron brace dampers revealed unexpectedly low sensitivity to the placement and, also, noticeably higher reliability than the diagonal dampers. On the other, hand while comparing the acceleration reductions, the chevron brace dampers were less effective and also less reliable than the diagonal dampers.

4.1.4. Structural models with hybrid friction-VE dampers

Table 11 illustrates the percentage reductions in the peak values of the tip deflection experienced by the structures fitted with the hybrid friction-VE dampers compared with results of the undamped structures. The dampers achieved satisfactory average reductions under the Kobe, Northridge and San Fernando earthquakes, whereas the reductions experienced under the El Centro and Hachinohe earthquakes were only moderate. In the case of the El Centro, Hachinohe and Northridge earthquakes, the highest average deflection reductions were obtained when the dampers were placed in the storeys 13 to 15 while in the case of the Kobe and San Fernando earthquakes, it was when the dampers were placed in the lowest storeys.

The percentage reductions in the peak values of the tip acceleration experienced by the same structures are illustrated in Table 12. The range of the results was unexpectedly wide varying from an average reduction of 15.3% obtained under the El Centro earthquake to a poor 0.8% average reduction recorded under the Northridge earthquake. Clearly the highest reduction occurred in the structures with the dampers fitted in the storeys 4 to 6. The tip acceleration reductions for the other damper placements were considerably lower and also less consistent.

The results presented in Tables 11 and 12 show that the expected high and reliable performance of the hybrid friction-VE dampers was achieved only partially. It is evident that the structures embedded with the hybrid friction-VE dampers followed a similar trend to the structures fitted with the chevron brace friction dampers. This means that whereas the friction components of the hybrid dampers operated appropriately, the VE component remained essentially ineffective.

4.1.5. Structural models with VE dampers –lower toggle configuration

The percentage reductions in tip deflection for the lower toggle VE dampers are illustrated in Table 13. The highest average reduction of 18.8% was obtained under the Kobe earthquake, whereas the lowest average reduction of 7.9% occurred under the Hachinohe earthquake. In the cases of the El Centro and Hachinohe earthquakes, the highest average tip deflection reductions occurred when the dampers were placed in the uppermost storeys, while a gradual decrease in efficiency was experienced as the dampers were moved towards the bottom of the structure. A reverse trend occurred under the Kobe and San Fernando earthquakes with the dampers being more effective in the lower storeys and decreasing in efficiency as they were moved towards the top of the structure. In the case of the Northridge earthquake, the performance remained relatively consistent for all the placements.

The results for the same damping systems in terms of reduction in tip acceleration are presented in Table 14. The highest average reduction of 21.2% was achieved under the El Centro earthquake, while the lowest average reduction of 11.2% occurred under the Northridge earthquake. The dampers displayed extraordinary performance when placed in the storeys 1 to 6 and 13 to 15. In contrast, when fitted in the uppermost storeys, an increase in average acceleration by 6.5% was experienced.

Despite the fact that the VE damper was created to represent only 42% of the damping force of the diagonal VE damper, its overall performance was noticeably higher and also more reliable. The results for the reduction in tip deflection followed a trend relatively close to the one for the structures fitted with the chevron brace friction dampers. With regard to reductions in tip acceleration, the results comply with a trend which was closest to that of the diagonal VE dampers.

To provide extra comparisons, structures embedded with the lower toggle friction dampers were also analysed. The results revealed a noticeable level of similarity to those of the lower toggle VE dampers and for that reason are not presented in this paper. However, the time history graphs of both types of dampers make more obvious that amplifying force of the toggle brace assembly altered damping response of friction (or VE) dampers to operate in a relatively similar way.

4.1.6. Summary of finding in the 18-storey structural model

The overall results for an 18-storey frame-shear wall structure in terms of reduction in the peak values of the tip deflection are illustrated in Figs. 19-23. The highest reductions were recorded, as it was expected, for the structure fitted with the lower toggle VE dampers. The results reveal a high level of reliability under all excitations and when fitted in all the placements. The reductions obtained by the diagonal VE dampers were even higher at lower storeys; however their efficiency considerably decreases when moved towards the top of the structure. The most consistent performances in all placements and under all seismic excitations were revealed for both types of chevron brace dampers.

The hybrid friction-VE dampers acted in a similar way to that of the friction chevron brace dampers, which indicates that only the friction part of this damping system was working properly, while the VE part remained ineffective in most cases. Finally, the results of the diagonal friction dampers reveal the highest sensitivity to placement and also to variations in seismic excitations. These dampers achieved the highest reductions under the Hachinohe earthquake, which caused the highest structural deflections from all excitations. On the other hand, involvement of the diagonal friction dampers under the San Fernando earthquake excitation, which causes the lowest structural deflection, was rather unfavourable.

In the peak values of the tip acceleration for the same structure (Figs. 23-26), the highest reductions were recorded for the structure fitted with the diagonal VE dampers. The tip acceleration reductions of these dampers were greatest when placed in the lower storeys. The average reductions for lower toggle dampers were close to those of the diagonal VE dampers; however, their reductions for the lowest storey placements were noticeably lower. The diagonal friction dampers displayed once again the highest sensitivity to variation of the dampers placement and seismic excitations. The slightly lower overall tip acceleration reduction was attributed to their ineffectiveness in the uppermost storeys and particularly their poor effectiveness under the San Fernando earthquake excitation.

The hybrid friction-VE damper and the friction chevron brace dampers followed similar trends with rather inconsistent acceleration reductions under the El Centro, Hachinohe and Kobe earthquakes while the reductions under the Northridge and San Fernando earthquakes were quite small. The lowest tip acceleration reduction was displayed for the chevron brace VE dampers where satisfactory reductions were recorded only under the El Centro earthquake excitation.

As the results for the diagonal friction damper were inconsistent, a combined damping system consisting of the diagonal friction damper placed in the 16th storey and the diagonal VE damper placed in the 1st storey was also analysed under all the earthquake excitation. The results are presented in Table 15 and it can be seen that there are significant reductions in both the investigated parameters under all 5 earthquake excitations. Furthermore, to emphasize the significance of these results, it should be pointed out that this combined damping system consisted of only two dampers.

4.2 12-storey models

The second type of medium rise structure which was investigated in this paper was represented by the 12-storey frame-shear wall model (see Fig.2). The results of this structure under five earthquake excitations are presented below.

4.2.1. Undamped structural model

An undamped structural model was again considered in order to compare its results with the results of the structures fitted with the damping systems. The tip deflection and tip acceleration of this structure experienced under five earthquake excitations can be seen in Table 16.

4.2.2. Structural models with friction and VE dampers – diagonal configuration

The percentage reductions in the peak values of the tip deflection experienced by the structures fitted with the diagonal friction dampers are presented in Table 17. The dampers display a very high level of efficiency in most cases. The highest average reduction of 27.9% was obtained under the El Centro earthquake and even the lowest overall reductions achieved under the Kobe earthquakes were reasonably high. The dampers placed in the lowest storeys produced in the majority of cases, only

minor tip deflection reductions; on the other hand the deflection reductions were significantly higher when the dampers were placed in the storeys with the higher interstorey drifts (Table 18).

Percentage reductions in tip deflection for the same structure fitted with the diagonal VE dampers are illustrated in Table 19. Clearly the highest performance was achieved under the El Centro earthquake with an exceptional average reduction of 29.6%. The average deflection reduction that occurred under the Kobe earthquake was also reasonably high. However, the reductions under the San Fernando and Hachinohe earthquakes were only moderate and there were only minimal reductions under the Northridge earthquake. The results show very high average deflection reductions for the structure with the dampers located in the lower and middle storeys, while moving the dampers towards the uppermost storeys resulted in noticeably lower performance.

The results of tip acceleration reduction for the structures fitted with both damping systems are illustrated in Tables 20 and 21. The highest acceleration reductions can be observed when the dampers were placed in the lowest storeys, while their repositioning towards the top of the structure caused a gradual decrease in acceleration reductions.

The presented results once again confirmed patterns indicating that tip deflection reductions for the structures fitted with the diagonal friction dampers were gradually increased as the dampers were moved toward the top of the structure, whereas this trend was reversed for structures fitted with diagonal VE dampers. The highest tip acceleration reduction for both damping systems was achieved when the dampers were placed in the lowest storeys and gradually decreased as they were moved toward the top of the structure.

4.2.3. Structural models with friction and VE dampers – chevron brace configuration

The percentage reductions in tip deflection for the structures fitted with chevron brace friction dampers are illustrated in Table 22. The best performance, with an average deflection reduction of 21.5%, was obtained under the El Centro earthquake, this was followed by still adequately high reductions occurred under the Kobe, Northridge and San Fernando earthquakes. Conversely, the reductions displayed under the Hachinohe earthquake were rather insignificant.

The highest average deflection reduction occurred when the dampers were placed in the storeys 7 and 8. Consequent repositioning of these dampers towards the top of the structure caused slight decreases in efficiency, whereas the decrease in efficiency was much stronger as the dampers were repositioning towards the bottom of the structure.

Deflection reductions for the same structures fitted with the chevron brace VE dampers are displayed in Table 23. Clearly the best performance with an average reduction of 18.2% was obtained under the Kobe earthquake. The reductions occurred under the El Centro, Northridge and San Fernando earthquakes were still reasonably high, whereas the reductions experienced under the Hachinohe earthquake were yet again insignificant. A gradual increase in tip deflection can be seen as the dampers were moved from the bottom to the top of the structures. The deflection increases that occurred under the El Centro, Northridge and San Fernando earthquakes were also accompanied by a noticeable level of regularity, whereas the reduction for the Hachinohe and Kobe earthquakes remained in a relatively narrow range throughout all placements.

Percentage reductions in tip acceleration for the chevron brace friction dampers are illustrated in Tables 24. The results revealed high acceleration reductions obtained under the Kobe earthquake, however the reductions occurred under the other earthquakes were noticeably poorer. Clearly, the worst results occurred under the San Fernando earthquake with increase in average tip acceleration by 54.6%.

The reduction in tip acceleration experienced by the structures fitted with the chevron brace VE dampers are presented in Table 25. The results followed a trend similar to that of the structure fitted with the chevron brace friction dampers. The average tip acceleration reduction occurred under the Kobe earthquake was very high. Nevertheless, the reductions that occurred under the other earthquakes were clearly lower. The poorest results were recorded under the San Fernando earthquake, with an increase in the average acceleration of 36.6%.

In terms of damper placement, both types of dampers displayed some common features. The average tip acceleration reductions showed unfavourable increases for the all damper placements. However, the lowest increase for both types of dampers occurred when the dampers were placed in the

storeys 5 and 6, while the highest were experienced when the dampers were placed in the uppermost storeys.

The overall reductions in tip deflection for the chevron brace dampers were equally high compared to those of the diagonal dampers. The reductions in tip displacement for both types of the chevron brace dampers revealed a lower level sensitivity to the placement and a higher consistency than the diagonal dampers. On the other hand in terms of acceleration reduction, both types of the chevron brace dampers were the least effective damping systems which in most cases created unfavourable results.

4.2.4. Structural models with hybrid friction-VE dampers

The percentage reductions in the peak values of the tip deflection experienced by the structures fitted with hybrid friction-VE dampers are illustrated in Table 26. The highest performance occurred under the El Centro earthquake with an average reduction of 18.4%. Damper performances obtained under the other earthquakes were noticeably lower and the lowest average reduction of 6.5% was recorded under the Northridge earthquake.

The dampers experienced a consistent performance in the all placements. However, their effectiveness was slightly higher when fitted in the lower storeys. In the case of the El Centro and Kobe earthquakes tip deflection reductions gradually increased as the dampers were moved from the top to the bottom of the structures, while under the Northridge and San Fernando earthquakes this trend was reversed. The reductions occurred under the Hachinohe earthquake were consistent over the all placements.

Table 27 presents the percentage reduction in tip acceleration for the same structure. The highest average reduction of 19.6% occurred under the Hachinohe earthquake. The reductions experienced under the Northridge and Kobe earthquakes were noticeably lower, although still relatively high. The lowest reductions (including some increases in acceleration) occurred under the El Centro and San Fernando earthquakes. The highest tip acceleration reductions occurred when the dampers were fitted in the storeys 3 and 4, in contrast, the least effective were in the top storeys. In the case of the El Centro earthquake, the dampers were effective only in the lowest storeys.

From the results it is clear that the structures fitted with the hybrid friction-VE dampers followed the pattern relatively close to that of the structures fitted with the diagonal VE dampers. Based on the presented results, it is suggested that whereas the VE part of the hybrid damper operated appropriately, the friction part remain rather ineffective. The illustrated high efficiency of the diagonal VE part and the inefficiency of the chevron brace friction part of the hybrid damper were in direct contrast to the hybrid damper fitted in the 18-storey structures (where only the chevron brace friction dampers operated effectively). Contrast in performances make it obvious that creating a hybrid friction-VE damper is rather complex and so requires a more comprehensive study.

4.2.5. Structural models with VE dampers –lower toggle configuration

The percentage reduction in tip deflection for the structures fitted with the lower toggle VE dampers are presented in Table 28. The dampers show a high performance under the all earthquake excitations. The highest average reduction of 21.8% occurred under the El Centro earthquake. High average deflection reductions were also recorded under the other earthquakes and even the lowest average reduction recorded under the Northridge earthquake reached a value of 11.9%.

While considering the efficiency of the placements, the highest average deflection reduction was obtained by the structures with the dampers fitted in the storeys 3 and 4. From Table 28 it can also be seen that under the Northridge and San Fernando earthquakes, damper efficiency increased from the bottom to the top of the structures, while under the El Centro earthquake reverse trend was experienced. In the case of the Kobe earthquake, the dampers performed significantly better in the lower storeys while in the case of the Hachinohe earthquake, the results were rather complex and did not follow any obvious pattern.

The percentage reductions in tip acceleration for the same structures are presented in Table 29. Despite a convincing overall performance a wide range of results was experienced. The tip acceleration varied from a 3.4% average increase, experienced under the San Fernando earthquake, to 21.8% average reduction obtained under the Hachinohe earthquake. The highest average acceleration

reduction occurred when the dampers were fitted in the storeys 9 and 10 while in contrast a significant increase in acceleration occurred when the dampers were fitted in the uppermost storeys.

4.2.6. Summary of finding in the 12-storey structural model

The overall results of all damping systems for the 12-storey structure in terms of reduction in the peak values of tip deflection (Figs. 27-32) were significantly high, with an exceptionally narrow interval of overall performance. On the other hand, the range of particular reductions remained relatively wide.

The highest tip deflection reductions and also the most consistent performance were obtained, yet again, for the lower toggle dampers. The tip deflection reductions for the diagonal friction dampers were generally comparable to those of the lower toggle VE dampers; however, in a few cases, this remained rather ineffective. Slightly lower overall deflection reductions for both the chevron brace dampers as compared to the diagonal friction dampers were due to their poor performances under the Hachinohe earthquake. The widest range of results was displayed for diagonal VE dampers. However, their overall reduction also remained at an adequately high level. The reductions for the hybrid friction-VE dampers were comparable to those of the other damping systems. However, their results suggested that, whereas the VE part of damping system operated effectively, the friction part of this damping system remained rather ineffective.

Whilst in terms of tip deflection reduction for the 12-storey structure, all damping systems performed exceptionally well, the results in terms of the peak values of tip acceleration reduction were considerably poorer (Figs. 31-34). The highest reductions were recorded for the lower toggle VE dampers. However, even these dampers remained unreliable under the San Fernando earthquake. The reductions for the diagonal VE dampers were rather inconsistent with an increase in tip accelerations under the Northridge earthquake. The reductions for the hybrid friction-VE damper were generally high except for the El Centro and San Fernando earthquakes where slight increases in acceleration were recorded. The tip acceleration reductions of the diagonal friction dampers were uneven and in many cases rather insufficient. Clearly the poorest results with strong increase in tip acceleration were recorded for the chevron brace VE dampers and chevron brace friction dampers which performed effectively only under the Kobe earthquake.

Similar to what was done in the case of the 18-storey structure, a combined damping system, which consisted of the diagonal friction damper placed in the 11^{th} storey and the diagonal VE damper placed in the 1^{st} storey was also analysed. The results presented in Table 30 demonstrate significant tip deflection and tip acceleration reduction under all earthquake excitations.

5. Discussion and conclusion

This comprehensive study treated seismic mitigation by using six different damping systems, namely friction and VE diagonal dampers, friction and VE chevron brace dampers, hybrid friction-VE dampers and lower toggle VE dampers. These damping systems were embeded into six different placements (one at a time) within cut outs of shear walls to mitigate the seismic response of medium-rise building structures. Finite element techniques were used to model the dampers and the structures to obtain the dynamic responses under five different earthquake excitations, using time history analyses. Damper properties such as stiffness, damping coefficient, location, configuration and size were varied and results for tip deflections and accelerations were obtained.

Despite the availability of sophisticated computer facilities, calculating the type of damping devices and their optimal placement and size still remains highly an iterative trial and error process. What makes the problem even more difficult is the uncertainty of seismic inputs as the forces of nature can vary tremendously. The range of the results presented in this paper illustrates the complexity of the problem of optimization in the use of damping devices. Nevertheless, the overall performances of all damping systems were satisfactory and some useful features can be observed.

In the 18-storey structure reductions of up to 36% in the peak values of tip deflections and 47% in the peak values of the tip accelerations were obtained while in the 12-storey structure the highest tip deflection reduction was 43% and the tip acceleration reduction 50%

With regards to performance of particular damping systems, the friction dampers in the huge majority of cases surpassed the VE dampers in their ability to reduce the intensity of the initial strong strikes. In contrast, the VE dampers gradually decreased the deflection and acceleration of the structure. The performance of the friction dampers increased with higher interstorey drift, while the best performance of VE dampers was achieved when placed in the lowest storeys. In addition, the diagonal friction dampers performed better under the earthquakes which produced higher deflections of the structure. In contrast, the performance of these dampers under earthquakes that caused a lower structural deflection was less favourable. The performance of the diagonal VE dampers was noticeably less sensitive to this aspect. With regard to the reductions of the tip acceleration, both damping systems experienced the best performance in the lowest storeys, while their performance gradually decreased as the dampers were moved towards the uppermost storeys.

Despite the fact, that both types of the chevron brace dampers were created to represent only 66.6% of the damping force of the diagonal dampers, their overall tip deflection reduction was comparatively high and even significantly more reliable than those of the diagonal dampers. On the other hand, both types of chevron brace dampers were clearly the least effective in terms of tip acceleration reduction. The hybrid friction-VE dampers performed in a more stable and reliable manner than the diagonal and chevron brace dampers, nevertheless their overall reductions were in the majority of cases, slightly lower. The results of these dampers in an 18-storey structure indicated that only the friction part of the hybrid damper was operating properly; on the other hand in the 12-storey structure it was only the VE parts. The lower toggle VE damper displayed the highest performance and reliability from all damping systems. Despite the use of the VE damping mechanism, the trend in the tip deflection reductions of the lower toggle damper was similar to that of the chevron brace friction dampers.

A number of analyses of the two different structure types fitted with different damping systems and treated under different earthquake excitations were carried out to gain a better understanding of the effectiveness of the dampers and their placement. This study treated the structural response under a range of seismic excitations even when the dominant seismic frequencies matched the natural frequency of the structure.

A strategy for protecting buildings from earthquakes is to limit the tip deflection which provides an overall assessment of the seismic response of the structure. To this end, findings of the present study demonstrate that friction dampers are most effective when placed close to regions of the maximum interstorey drift, whereas VE dampers are most effective when placed in the lowest storeys. The combined damping system, which consist from the diagonal friction damper placed in the storey with the highest interstorey drift and the diagonal VE damper placed in the lowest storey is clearly more effective than the hybrid friction-VE dampers placed in the same cut outs. The relatively new configuration of lower toggle VE damper seems to be the best choice for seismic mitigation. This study has shown that it is possible to have seismic mitigation, under all earthquakes, by using certain damper types appropriately located within the structure. The large amount and variety of information generated in this study can enable the optimum use of dampers to mitigate seismic response in medium-rise building structures.

References

[1] Abbas, H. and Kelly, J.M. (1993), “A methodology for design of viscoelastic dampers in earthquake-resistant structures.” Technical report UCB/EERC-93/09, Earthquake Engineering Research Center, University of California, Berkeley.

[2] Abdullah, M.(1999), “Optimal placement of DVFC controllers on buildings subjected to earthquake loading,” Earthquake Engineering and Structural Dynamics, vol. 28, pp. 127-141.

[3] Aiken, I.D., Kelly, J.M. and Mahmoodi, P. (1990), “The application of VE dampers to seismically resistant structures.” Proc. 4th U.S. National Conf. on Earthquake Engineering. Palm Springs, California, Vol. 3, pp. 459-468.

[4] Ashour, S. A. and Hanson, R. D., (1987). “Elastic seismic response of buildings with supplemental damping,” Report No. UMCE 87-1, University of Michigan, Ann Arbour, MI.

[5] Constantinou, M.C., and Sigaher, A.N. (2000), "Energy dissipation system configurations for improved performance." Proceeding of the 2000 Structures Congress and Exposition, ASCE, May 8-10, 2000, Philadelphia, PA
[6] Constantinou, M.C., Soong, T.T. and Dargush, G.F. (1998), "Passive energy dissipation systems for structural design and retrofit." Monograph No.1, Multidisciplinary Center for Earthquake Engineering Research, State University of New York, Buffalo, N.Y.
[7] Constantinou, M. C. and Tadjbakhsh, I. G., (1983). "Optimum Design of a First Story Damping System," Computers and Structures, 17, 305-310.
[8] Hahn, G. D. and Sathiavageeswaran, K. R., (1992). "Effects of added-damper distribution on the seismic response of buildings," Computers and Structures, 43, 941-950.
[9] Hanson, R., (1993). "Supplemental damping for improved seismic performance," Earthquake Spectra, 9(3), 319-334.
[10] Hanson, R. D., Aiken, I., Nims, D. K., Richter, P. J., and Bachman, R., (1993). "State of-the-art and state-of-the-practice in seismic energy dissipation", ATC-17-1 seminar on seismic isolation, passive energy dissipation, and active control, San Francisco, CA, 449-471.
[11] Hisano, K., Kuribayashi, H. and Saitou, K, (2000). "The Application example of the hybrid friction-VE damper combined the hysteretic damper with viscous damper to high-rise building," Proc. 5th Inter. Conf. on Motion and Vibration Control, Sydney, Australia, Vol.1, pp. 451-456
[12] Kelly, J. M., Skinner, R. I., and Heine, A. J., (1972). "Mechanism of Energy Absorption in Special Devices for Use in Earthquake Resistant Structures," Bulletin of N. Z. Society for Earthquake Engineering, 5(3).
[13] Madsen, L.P.B., (2001) "Improving the seismic response of structures by the use of dampers in shear walls", ME thesis, School of Civil Engineering, Queensland University of Technology, Brisbane, Australia.
[14] Natke, H. G., (1993). "Topological Structural Optimization under Dynamic Loads", Optimization of Structural Systems and Applications, Eds. Hernandez, S. and Brebbia, C. A., Computational Mechanics Publications, Southampton, 67-78.
[15] Ray, D., Pister, K. S., and Chopra, A. K., (1974). "Optimum design of earthquake resistant shear buildings." Report No. UCB/EERC 74-3, Earthquake Engineering Research Center, University of California at Berkeley, Berkeley, CA.
[16] Ribakov, Y. and Gluck, J., (1999). "Optimal design of ADAS damped MDOF structures," Earthquake Spectra, 15(2), 317-330.
[17] Sadek, F., Mohraz, B., Taylor, W.A., and Chung, R.M. (November 1996), "Passive energy dissipation devices for seismic applications." Technical report NISTIR 5923. Building and Fire Research Laboratory, National Institute of Standards and Technology, Gaithersburg, Maryland 20899
[18] Shao, D., M.S., S.E., H. Kit Miyamoto, M.S., S.E. "Viscous damper versus friction damper for retrofit of a non-ductile reinforced concrete building with unreinforced masonry infill." SEAOC 1999 Convention
[19] Welch, P.D, "The use of fast Fourier transform for the estimation of power spectra: a method based on time averaging over short, modified periodograms." IEEE Trans. Audio Electroacoust. Vol.AU-15 (June1967) pp 70-73.
[20] Zhang, R. H. and Soong, T. T., (1992). "Seismic design of viscoelastic dampers for structural applications," Journal of Structural Engineering, 118(5), 1375-1392.

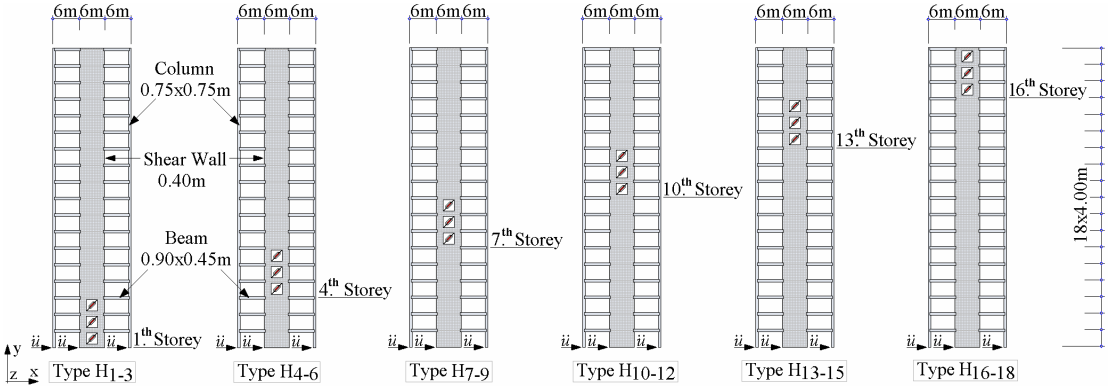

Fig.1 – Placement of dampers within 18-storey frame-shear wall structures.

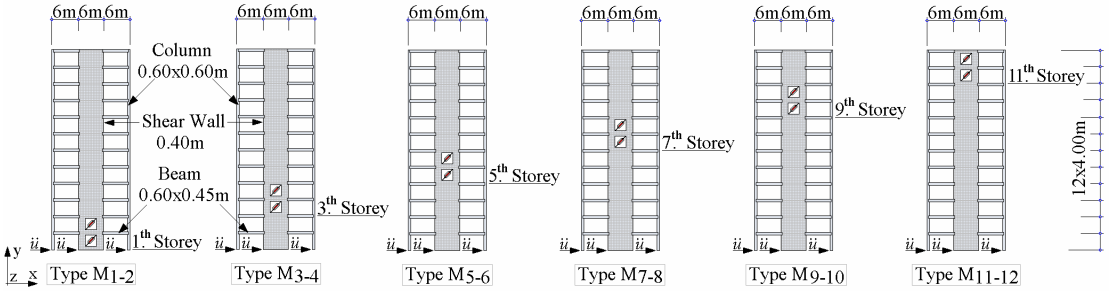

Fig.2 – Placement of dampers within 12-storey frame-shear wall structures.

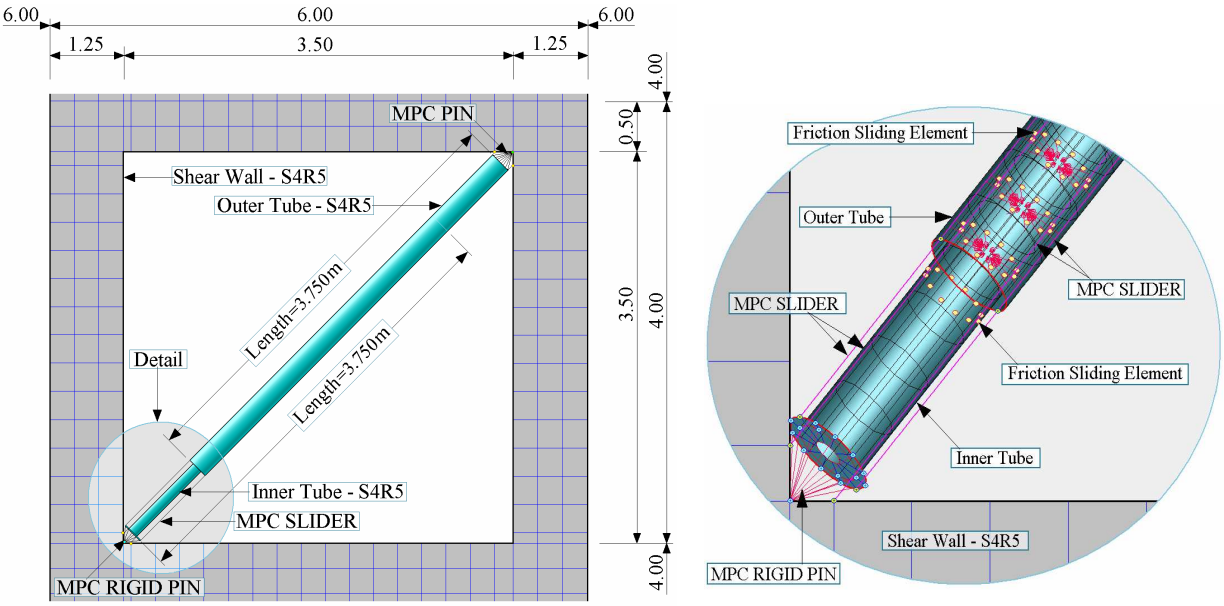

Fig.3 - Details of diagonal friction damper.

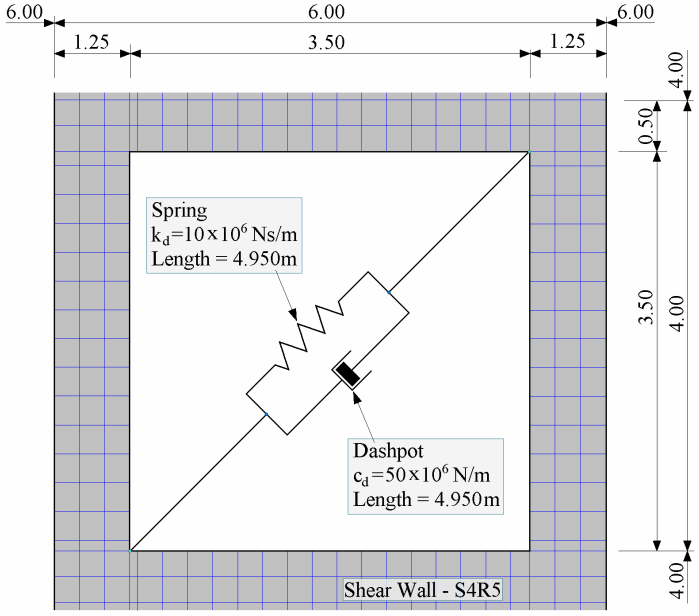

Fig.4 - Details of diagonal VE damper.

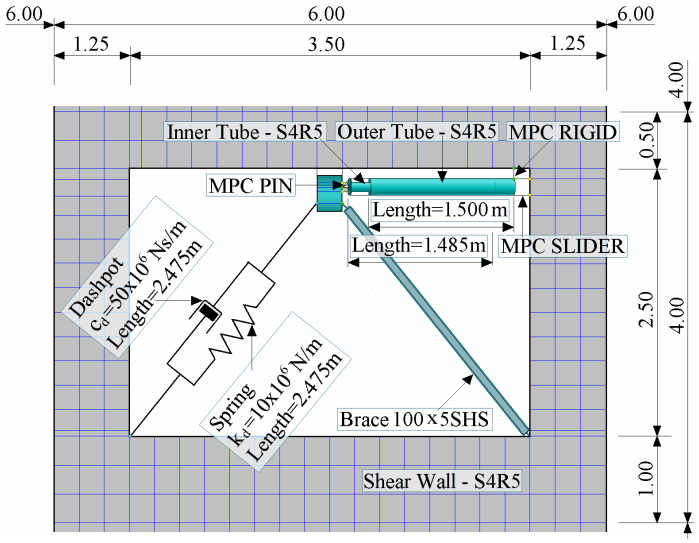

Fig.5 - Details of hybrid friction-VE damper.

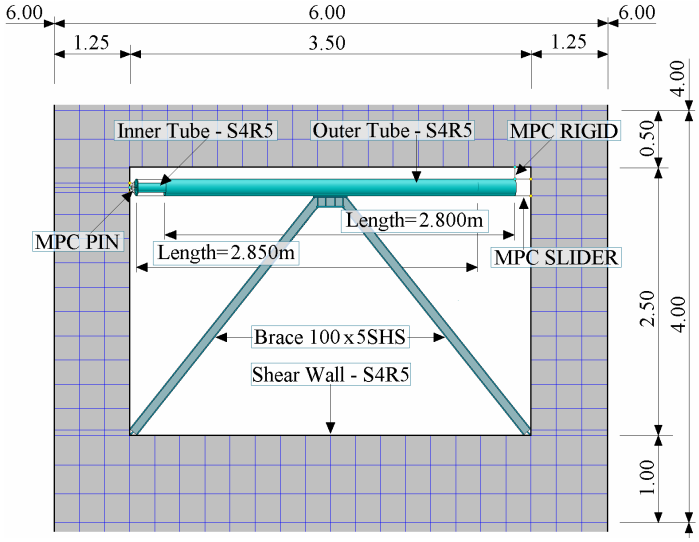

Fig.6 - Details of chevron brace friction damper.

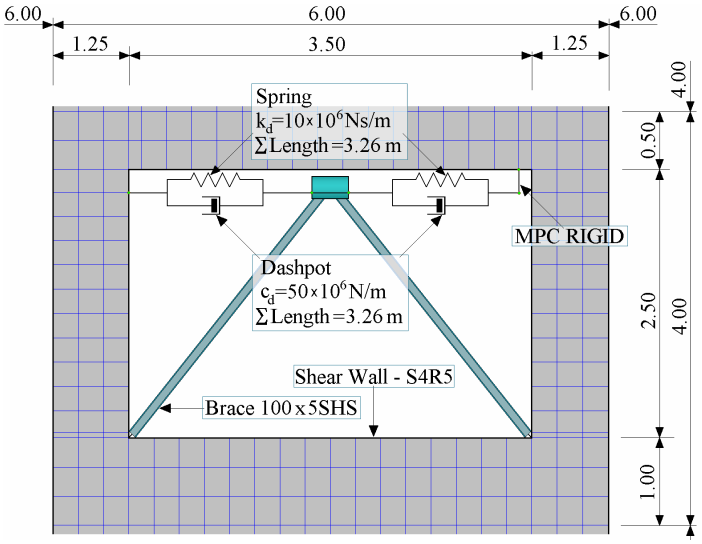

Fig.7 - Details of chevron brace VE damper.

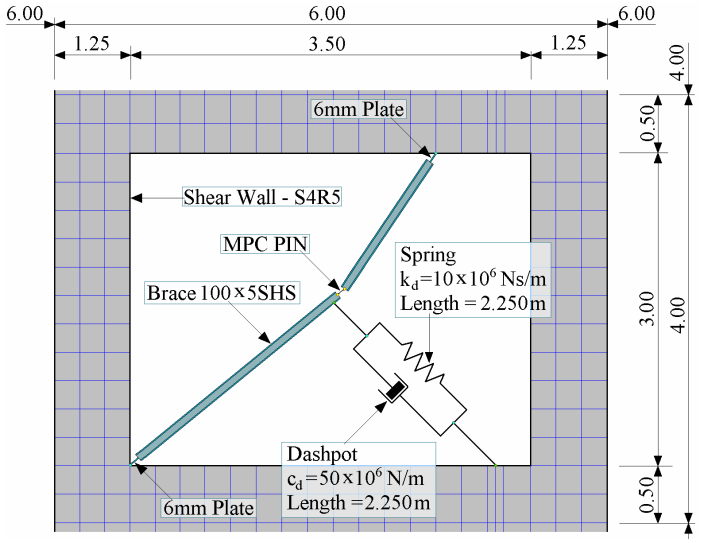

Fig.8 - Details of lower toggle VE damper.

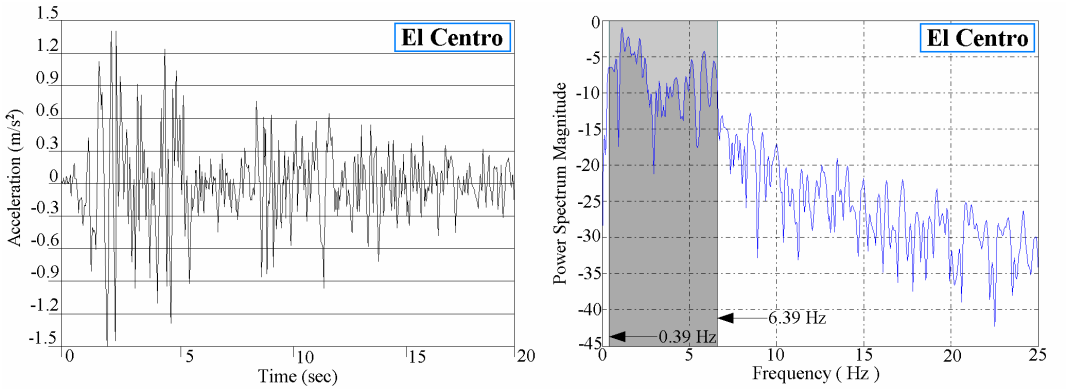

Fig.9 - El Centro earthquake record and its dominant frequencies.

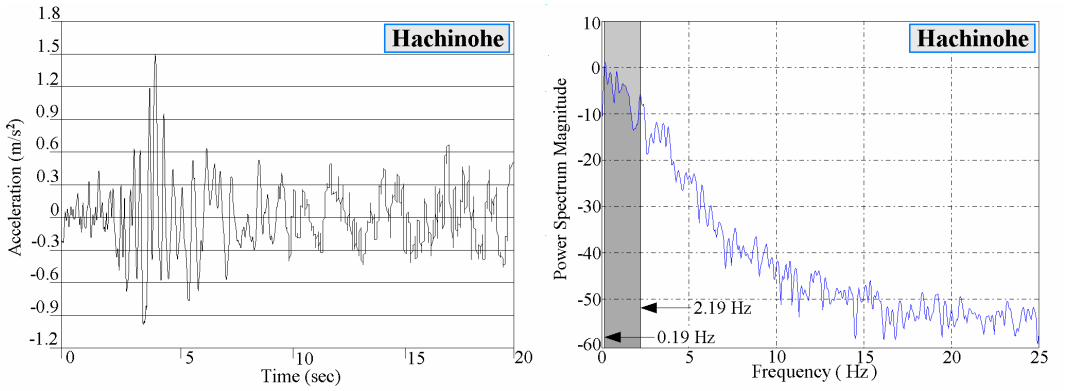

Fig.10 - Hachinohe earthquake record and its dominant frequencies.

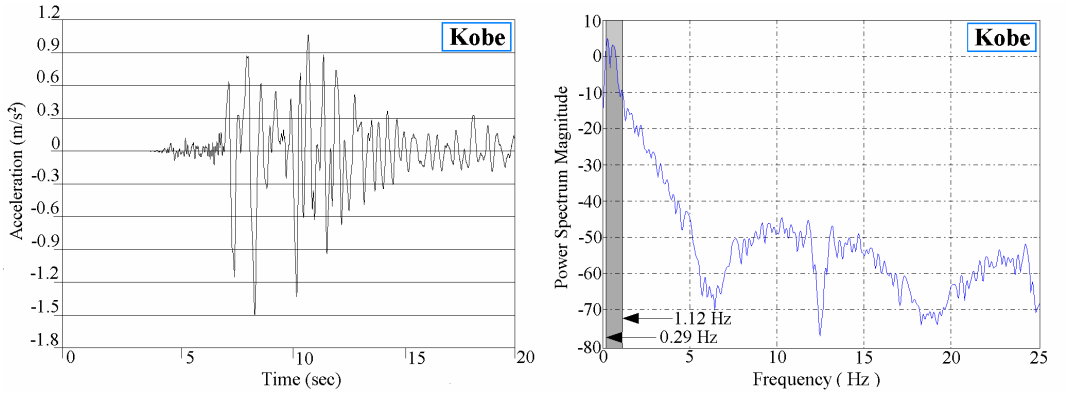

Fig.11 - Kobe earthquake record and its dominant frequencies.

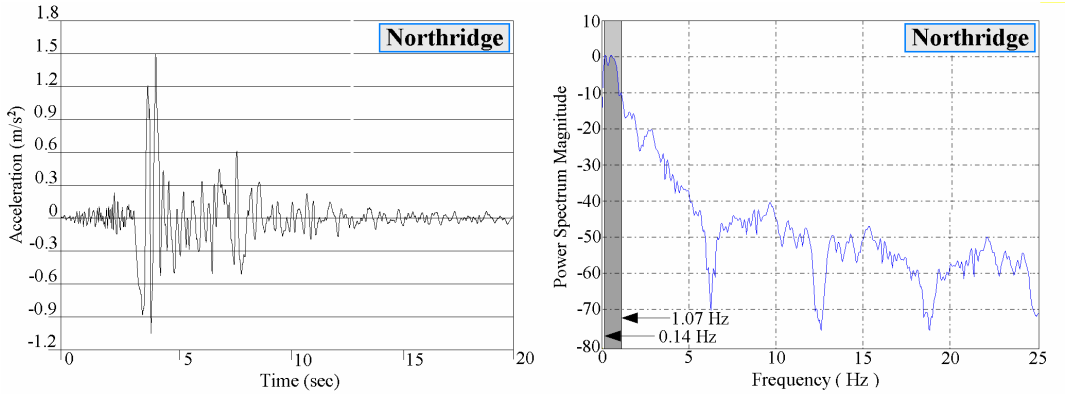

Fig.12 - Northridge earthquake record and its dominant frequencies.

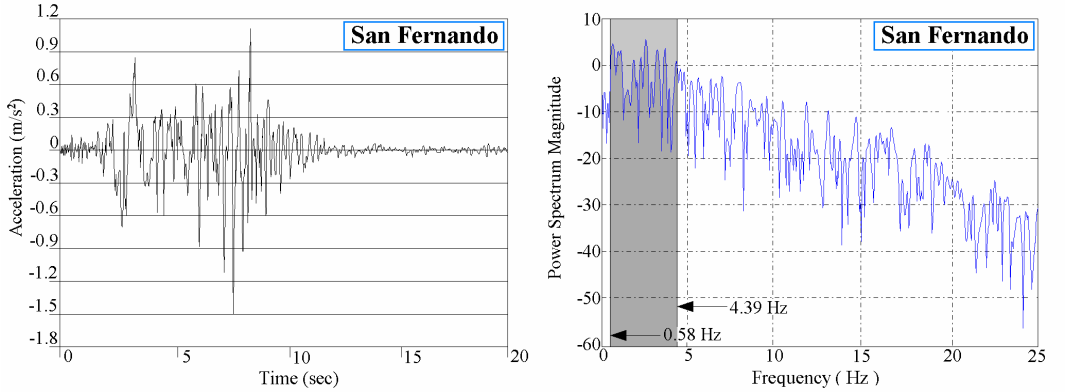

Fig.13 - San Fernando earthquake record and its dominant frequencies.

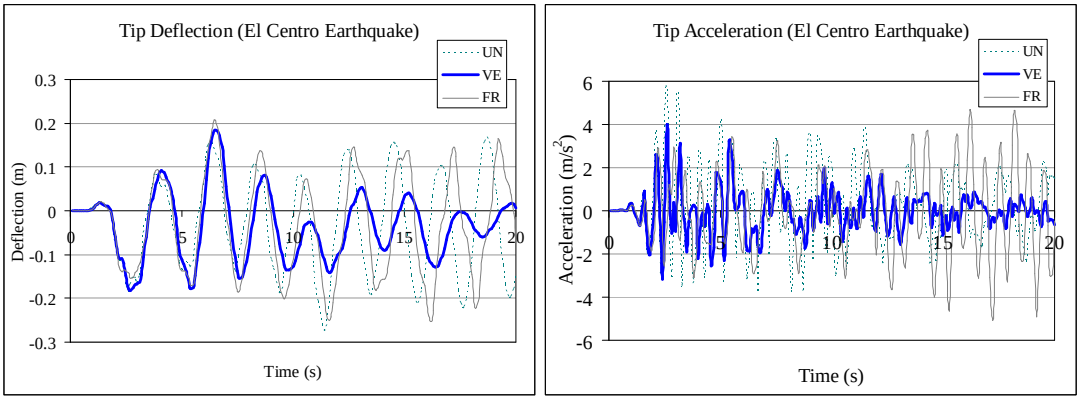

Fig.14 - Tip deflection and acceleration responses of H 1-3 structure fitted with diagonal VE and friction dampers and undamped structure under the El Centro earthquake.

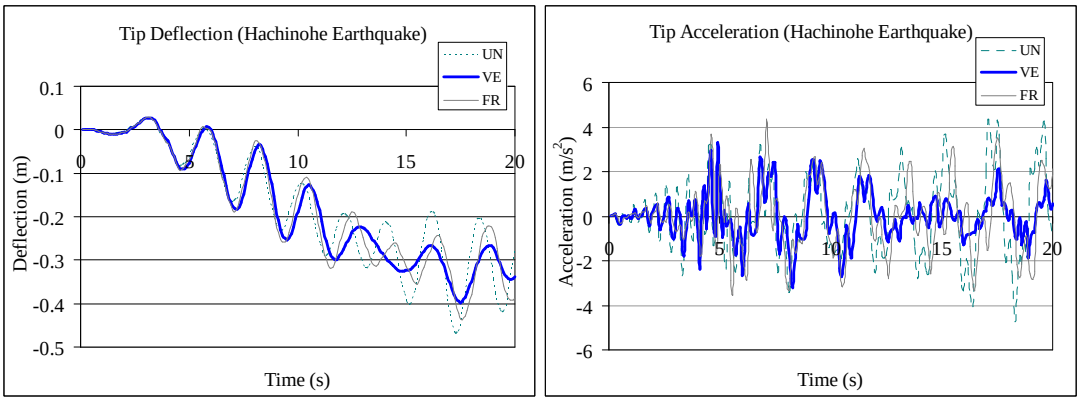

Fig.15 - Tip deflection and acceleration response of H 1-3 structure fitted with diagonal VE and friction dampers and undamped structure under the Hachinohe earthquake.

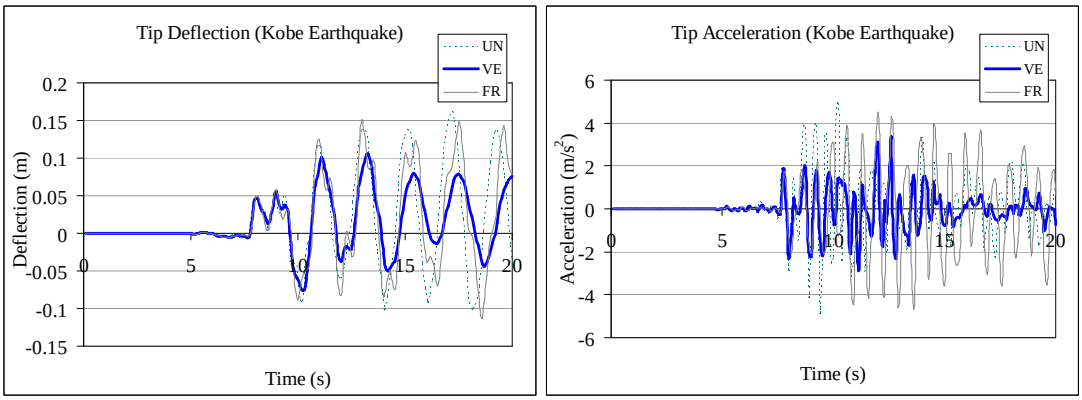

Fig.16 - Tip deflection and acceleration response of H 1-3 structure fitted with diagonal VE and friction dampers and undamped structure under the Kobe earthquake.

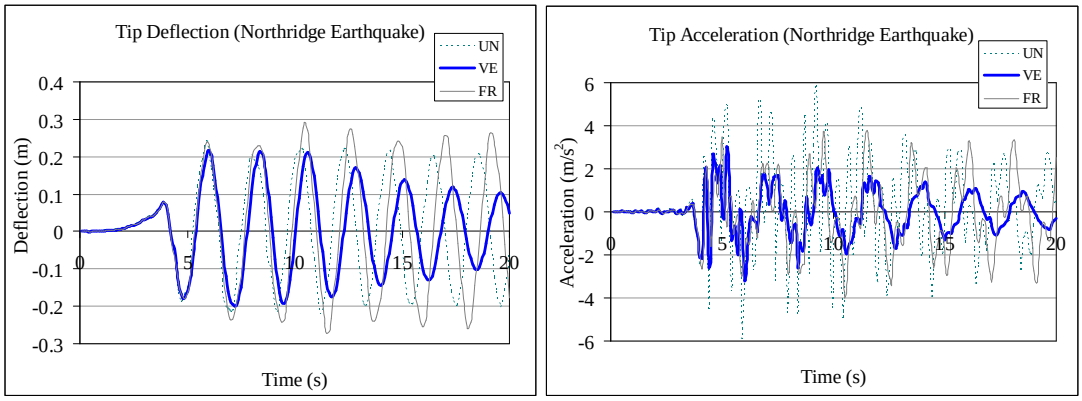

Fig.17 - Tip deflection and acceleration response of H 1-3 structure fitted with diagonal VE and friction dampers and undamped structure under the Northridge earthquake.

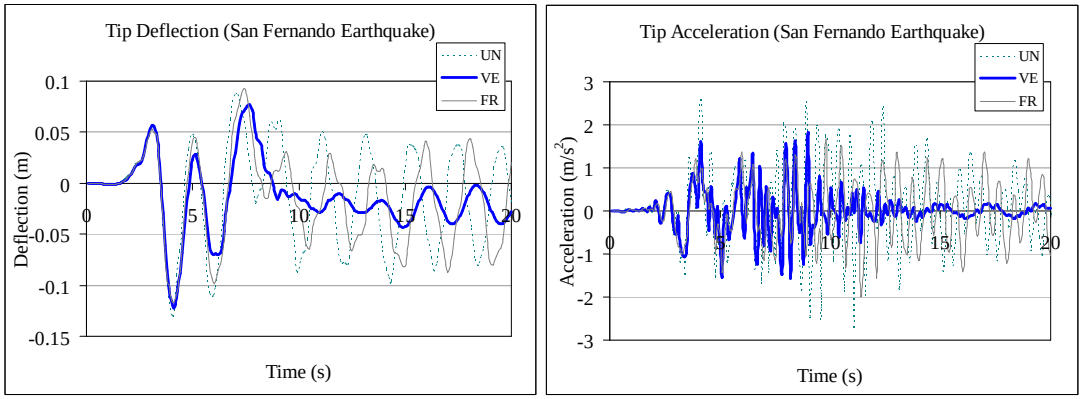

Fig.18 - Tip deflection and acceleration response of H 1-3 structure fitted with diagonal VE and friction dampers and undamped structure under the San Fernando earthquake.

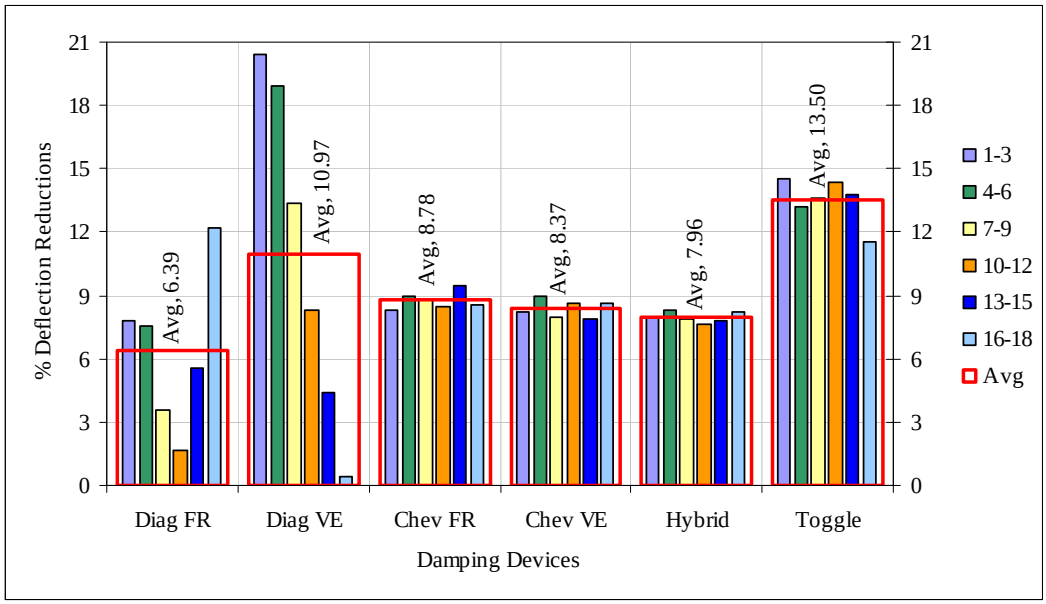

Fig.19 - Average percentage deflection reductions for all damping systems in all placements in 18-storey structure.

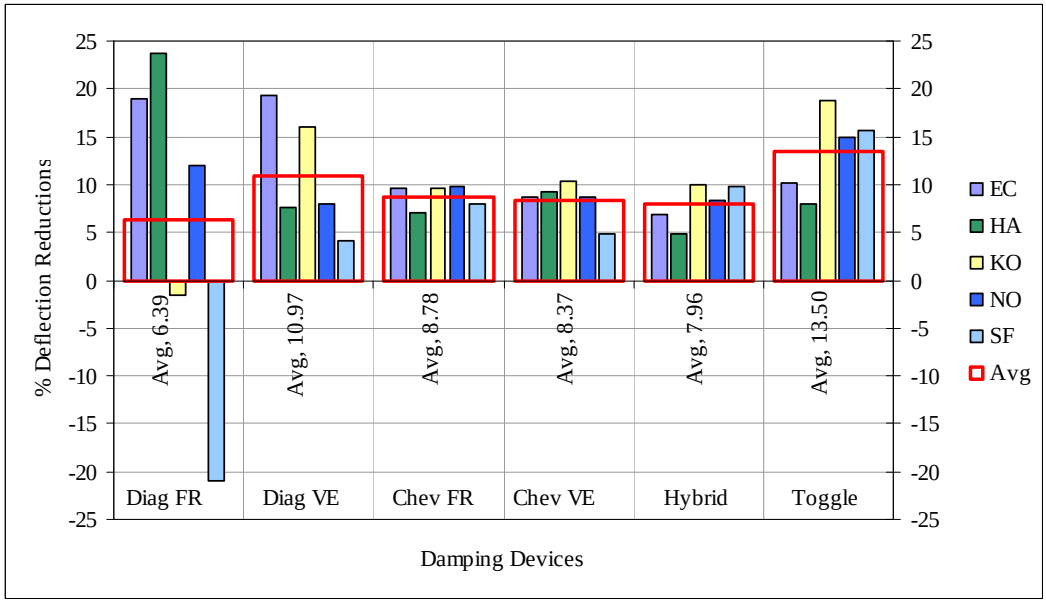

Fig.20 - Average percentage deflection reductions of all damping systems under different earthquake excitations in 18-storey structure.

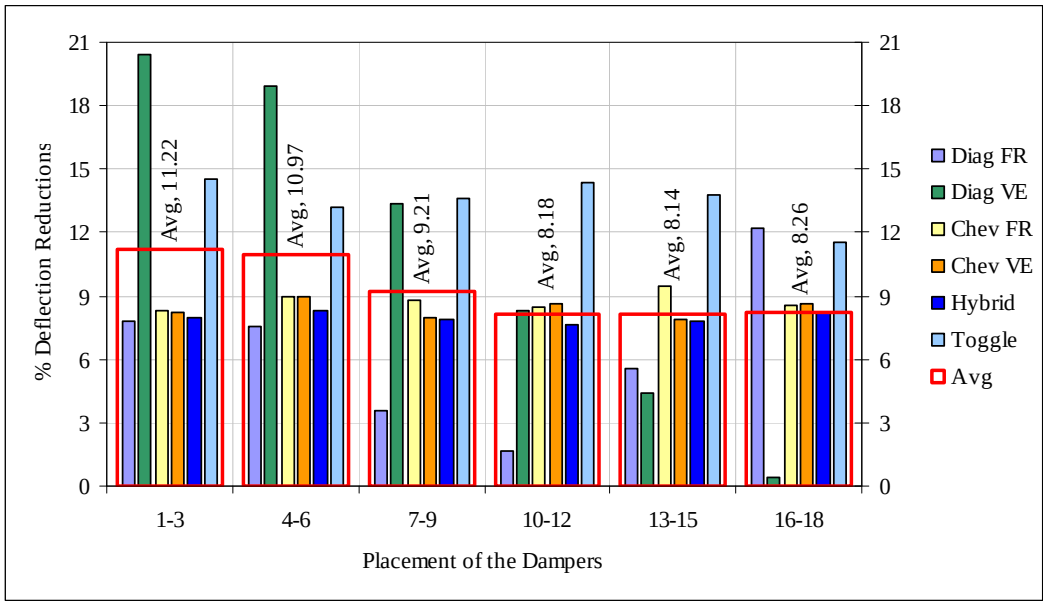

Fig.21 - Average percentage deflection reductions of all damping systems in terms of damper placement in 18-storey structure.

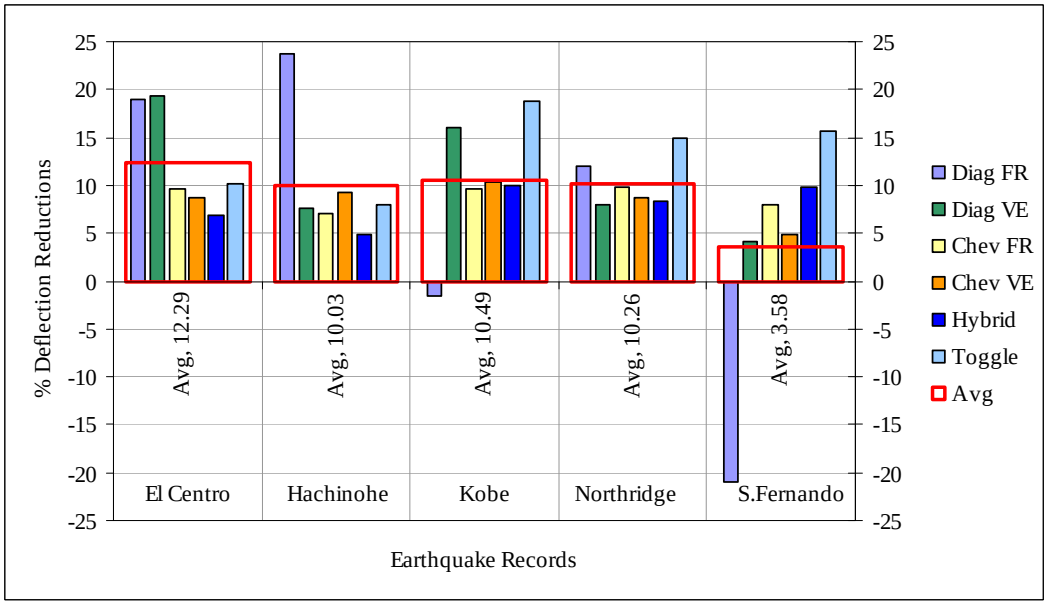

Fig.22 - Average percentage deflection reductions of all damping systems under different earthquake excitations in 18-storey structure.

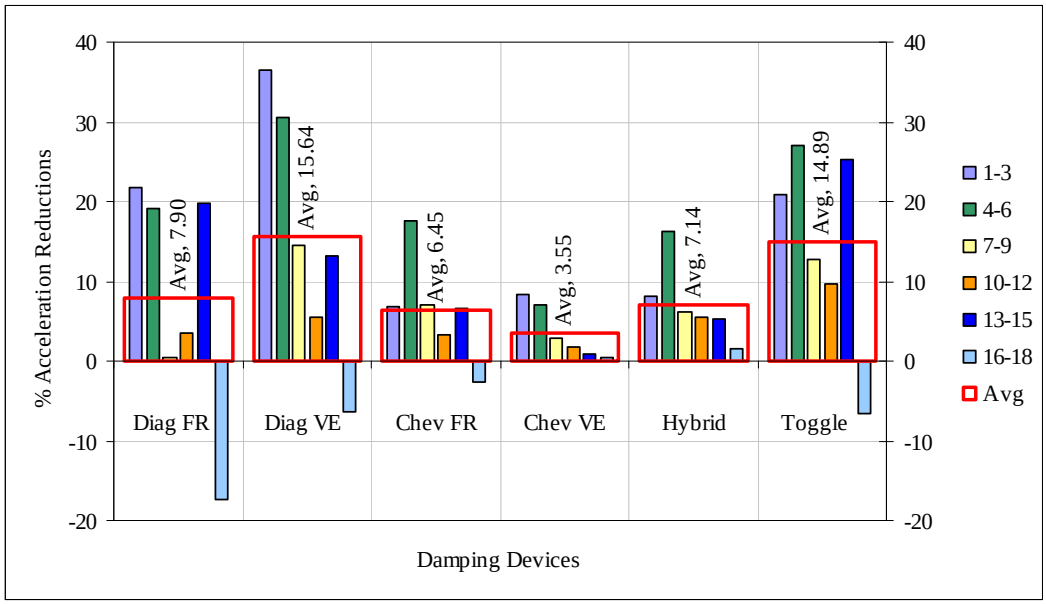

Fig.23 - Average percentage acceleration reductions for all damping systems in all placements in 18-storey structure.

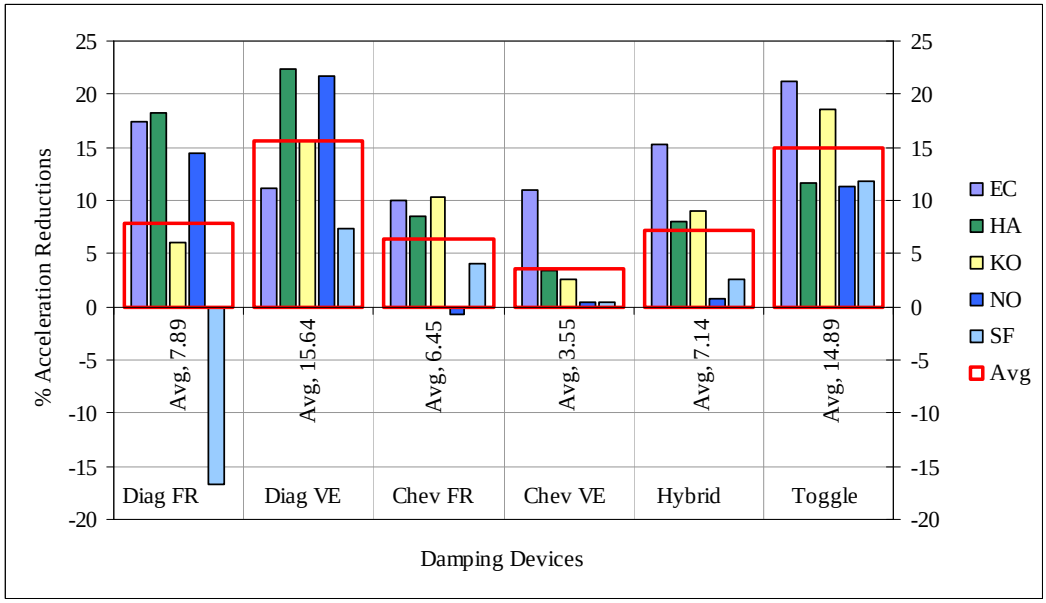

Fig.24 - Average percentage acceleration reductions of all damping systems under different earthquake excitations in 18-storey structure.

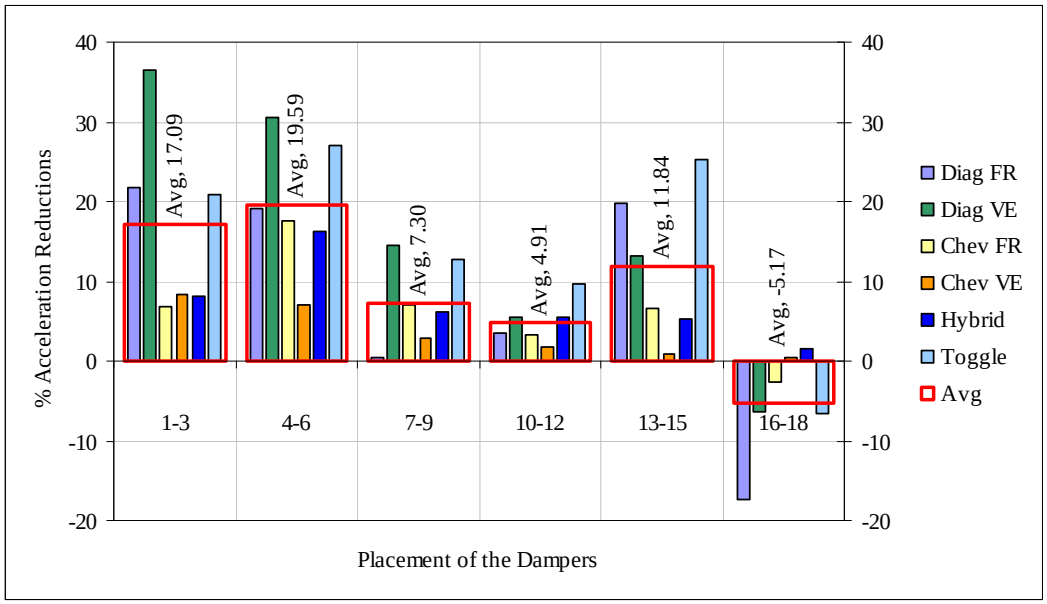

Fig.25 - 18-storey structure: Average percentage acceleration reductions of all damping systems in terms of damper placement.

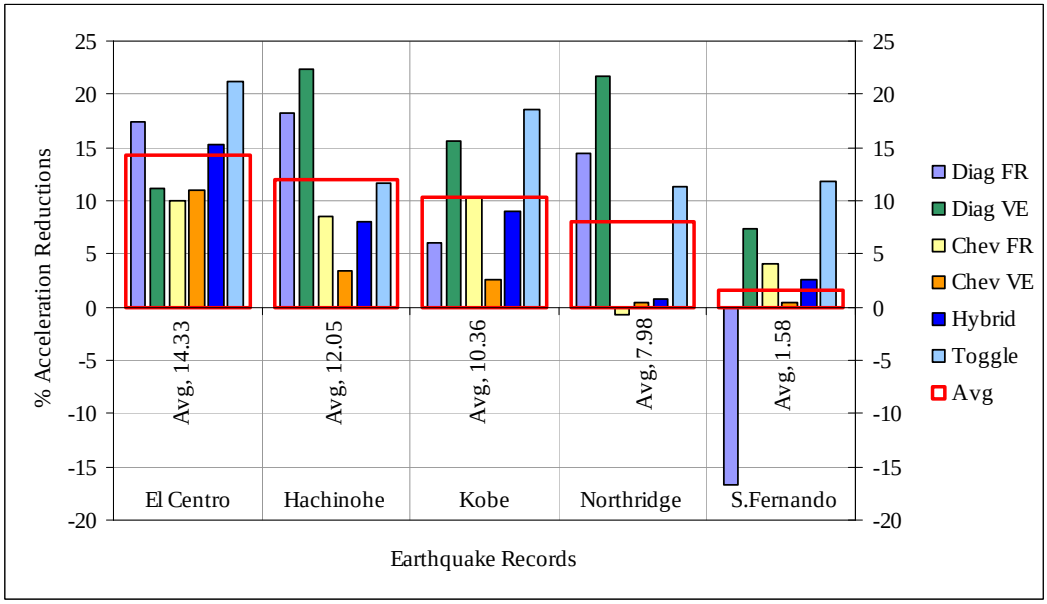

Fig.26 - Average percentage acceleration reductions of all damping systems under different earthquake excitations in 18-storey structure.

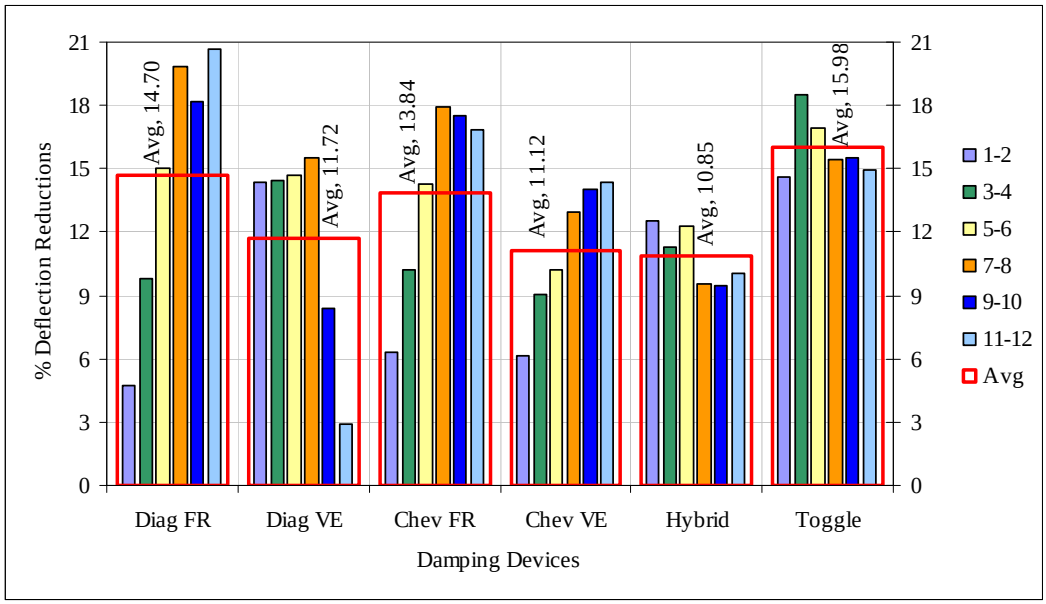

Fig.27 - Average percentage deflection reductions for all damping systems in all placements in 12-storey structure.

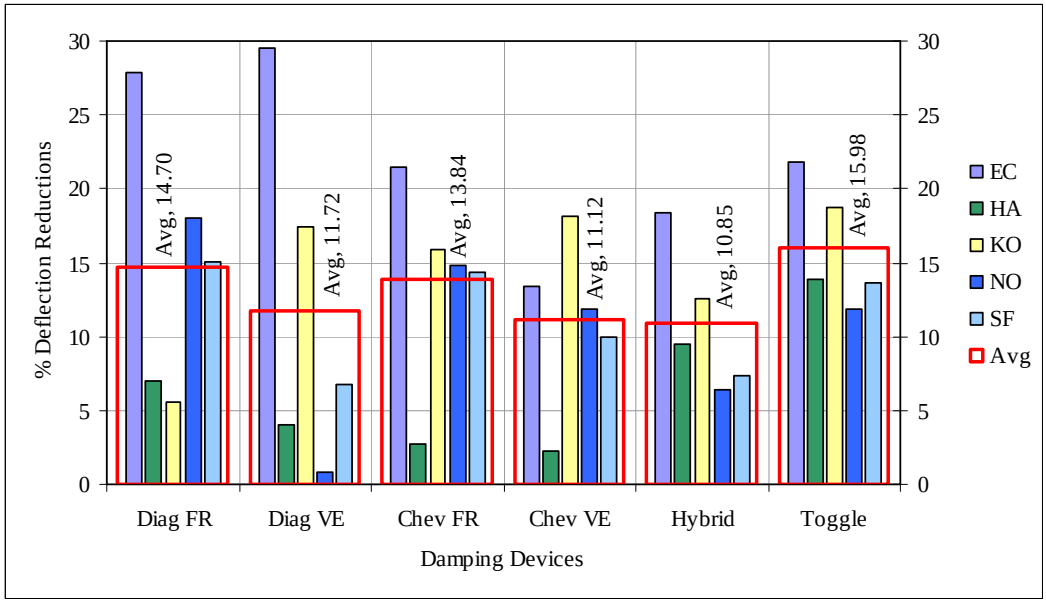

Fig.28 - Average percentage deflection reductions of all damping systems under different earthquake excitations in 12-storey structure.

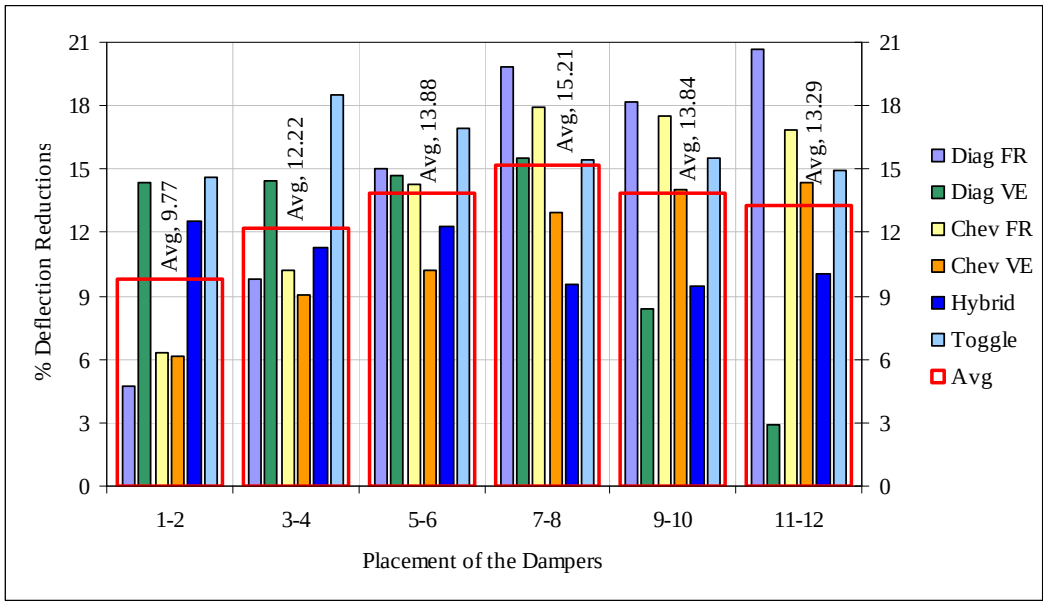

Fig.29 - Average percentage deflection reductions of all damping systems in terms of damper placements in 12-storey structure.

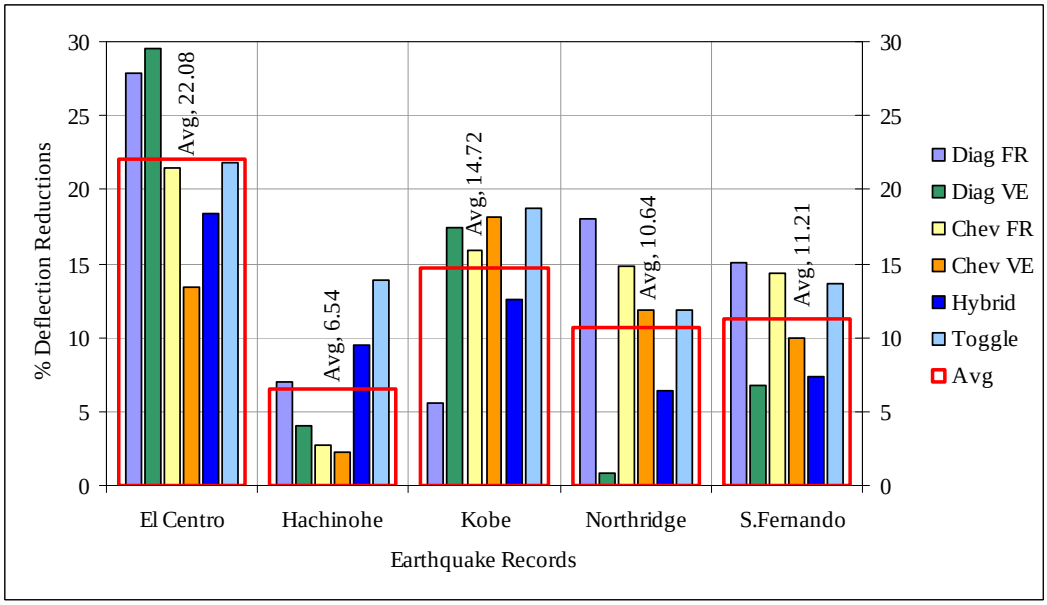

Fig.30 -: Average percentage deflection reductions of all damping systems under different earthquake excitations in 12-storey structure

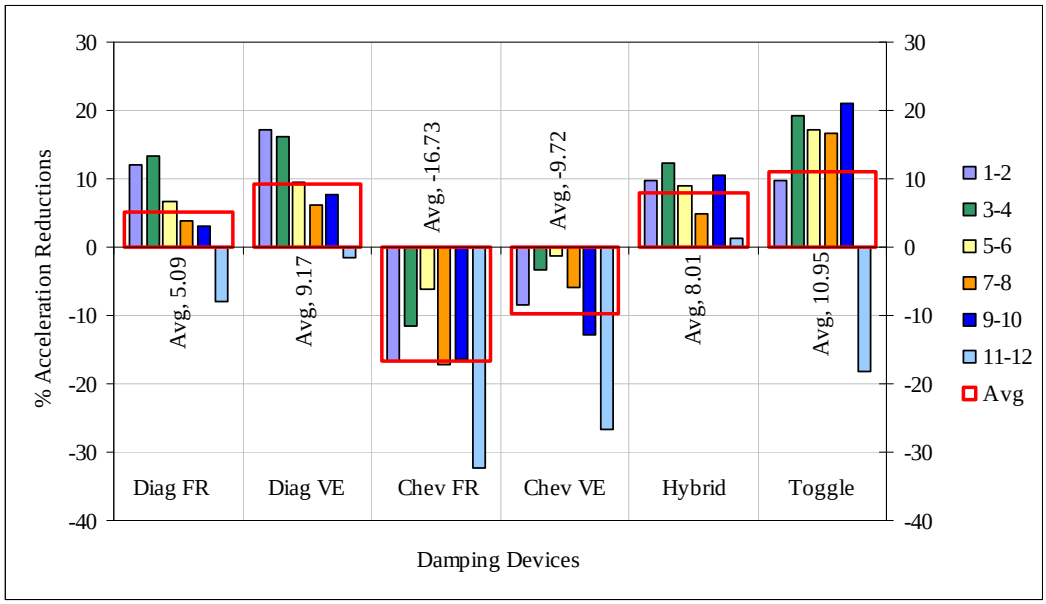

Fig.31 - Average percentage acceleration reductions for all damping systems in all placements in 12-storey structure.

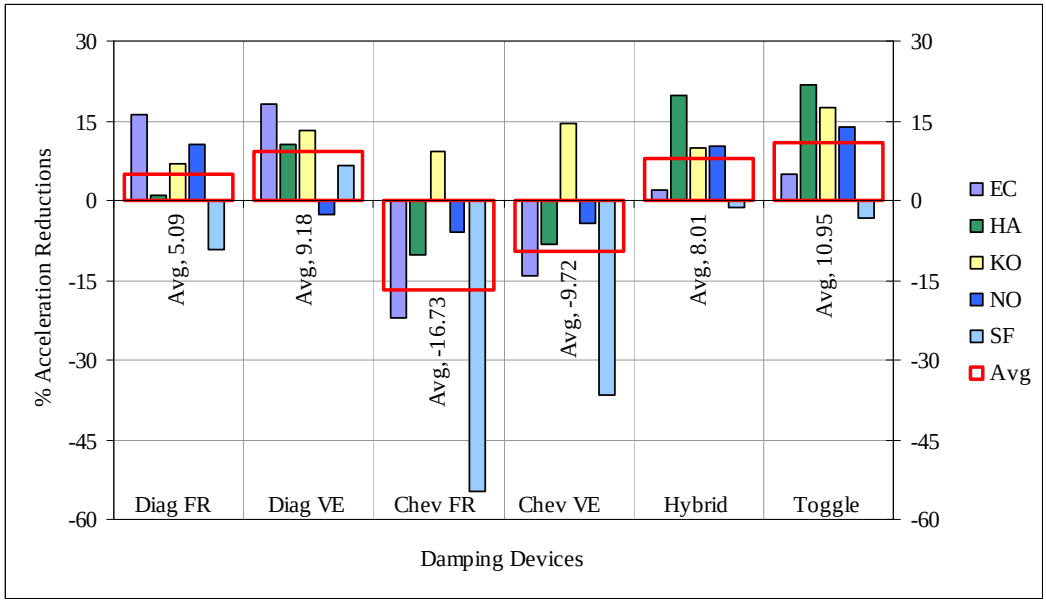

Fig.32 - Average percentage acceleration reductions of all damping systems under different earthquake excitations in 12-storey structure.

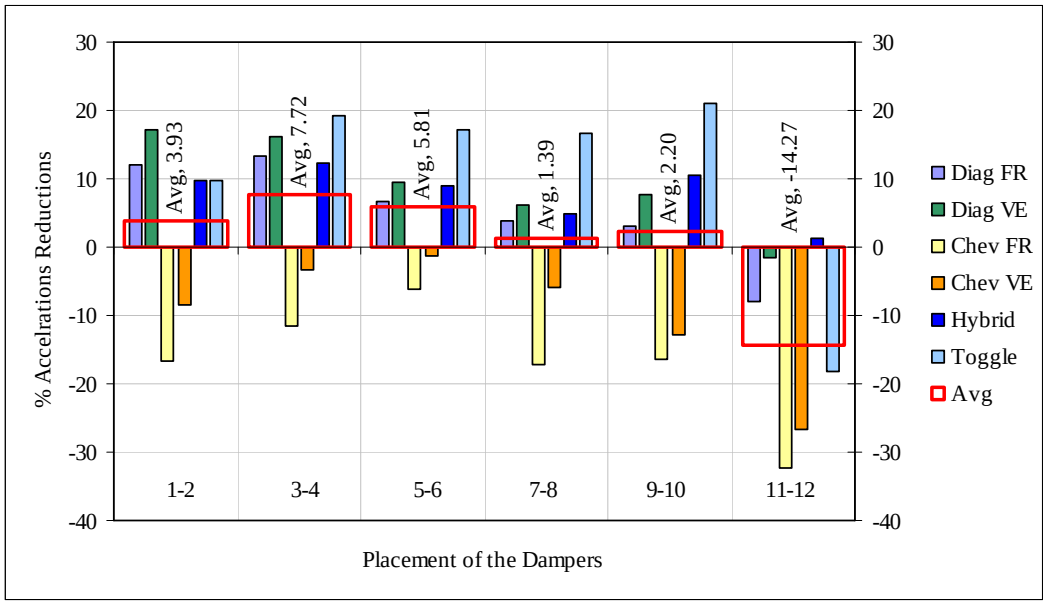

Fig.33 - Average percentage acceleration reductions of all damping systems in terms of damper placements in 12-storey structure.

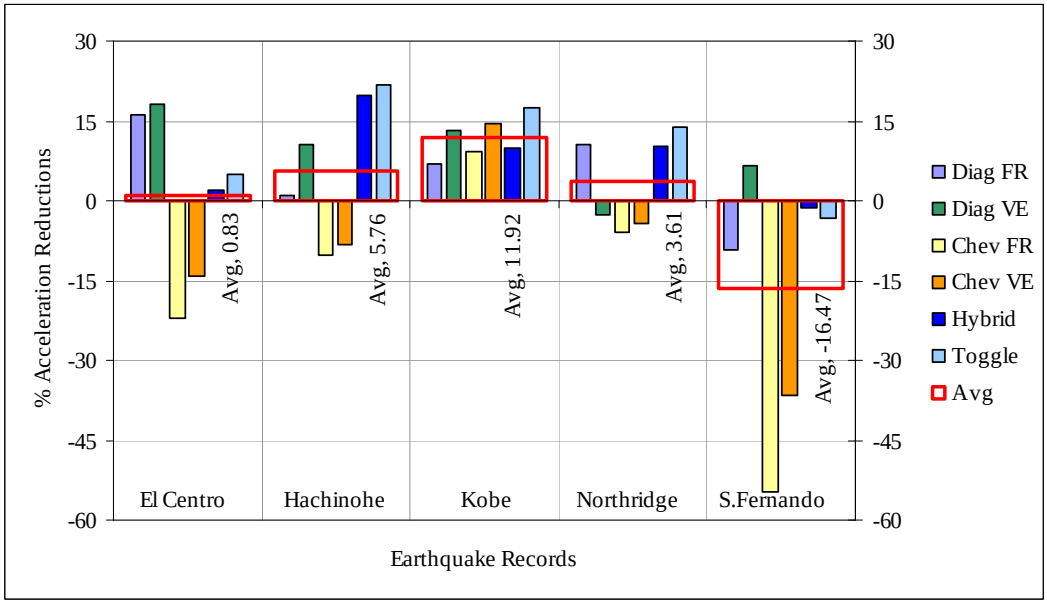

Fig.34 - Average percentage acceleration reductions of all damping systems under different earthquake excitations in 12-storey structure.

Table 1
Tip deflection and tip acceleration of the undamped 18-storey structure.

	El Centro	*Hachinohe*	*Kobe*	*Northridge*	*S.Fernando*
Deflection(m)	0.275	0.464	0.163	0.245	0.130
Acceleration(m/s^2)	5.66	4.72	4.93	5.95	2.72

Table 2
Percentage reductions in tip deflection of model with diagonal friction dampers

Model	*El Centro*	*Hachinohe*	*Kobe*	*Northridge*	*S.Fernando*	*Average*
H 1-3	14.55	13.48	13.50	-11.02	8.40	7.78
H 4-6	13.09	19.15	-7.36	11.43	1.53	7.57
H 7-9	17.09	28.37	-6.75	16.73	-37.40	3.61
H 10-12	22.55	26.24	-6.13	6.94	-41.22	1.67
H 13-15	24.36	25.53	-4.29	16.33	-34.35	5.52
H 16-18	22.18	29.08	1.23	31.43	-22.90	12.20
Average	18.97	23.64	-1.64	11.97	-20.99	6.39
Optimal	H13/19.10	H13/21.84	H1/5.21	H1/18.44	H4/4.86	H13/ 9.10

Table 3
Floors with largest interstorey drift

Drift	*El Centro*	*Hachinohe*	*Kobe*	*Northridge*	*S.Fernando*
1^{st} largest	14-15	11-12	14-15	16-17	13-14
2^{nd} largest	15-16	10-11	15-16	15-16	14-15
3^{rd} largest	16-17	12-13	16-17	14-15	12-13

Table 4
Percentage reductions in tip deflection of model with diagonal VE dampers

Model	*El Centro*	*Hachinohe*	*Kobe*	*Northridge*	*S.Fernando*	*Average*
H 1-3	33.09	15.60	35.58	11.84	6.11	20.44
H 4-6	33.82	12.06	28.22	13.47	6.87	18.89
H 7-9	20.36	8.51	24.54	8.16	5.34	13.38
H 10-12	12.73	4.96	14.72	5.31	3.82	8.31
H 13-15	8.00	2.13	3.07	4.90	3.82	4.38
H 16-18	7.64	2.84	-10.43	3.67	-1.53	0.44
Average	19.27	7.68	15.95	7.89	4.07	10.97
Optimal	H1/7.64	H1/3.19	H4/9.82	H1/2.45	H7/2.29	H1/ 4.53

Table 5
Percentage reductions in tip acceleration of model with diagonal friction dampers

Model	*El Centro*	*Hachinohe*	*Kobe*	*Northridge*	*S.Fernando*	*Average*
H 1-3	16.25	14.38	7.30	37.27	33.70	21.78
H 4-6	18.90	-1.48	26.98	30.86	20.51	19.16
H 7-9	13.43	40.80	-4.87	7.42	-54.95	0.37
H 10-12	23.14	17.34	7.30	5.23	-35.16	3.57
H 13-15	35.16	50.53	25.15	17.54	-28.94	19.89
H 16-18	-2.30	-12.26	-25.56	-11.30	-35.53	-17.39
Average	17.43	18.22	6.05	14.50	-16.73	7.90
Optimal	H16/14.65	H10/22.26	H1/9.54	H1312.28	H46.81	H4/ 4.07

Table 6
Percentage reductions in tip acceleration of model with diagonal VE dampers

Model	*El Centro*	*Hachinohe*	*Kobe*	*Northridge*	*S.Fernando*	*Average*
H 1-3	30.21	31.92	33.67	46.71	40.29	36.56
H 4-6	22.44	36.58	38.74	36.42	18.32	30.50
H 7-9	8.66	31.08	10.75	18.38	3.66	14.51
H 10-12	3.18	25.16	1.22	5.56	-7.33	5.56
H 13-15	8.30	10.78	15.42	20.74	10.62	13.17
H 16-18	-5.65	-1.27	-6.29	2.53	-21.61	-6.46
Average	11.19	22.37	15.58	21.73	7.33	15.64
Optimal	H4/6.01	H1/20.72	H1/12.78	H4/18.72	H7/9.16	H4/ 11.37

Table 7
Percentage reductions in tip deflection of model with chevron braced friction dampers

Model	*El Centro*	*Hachinohe*	*Kobe*	*Northridge*	*S.Fernando*	*Average*
H 1-3	4.71	-3.15	17.35	7.98	14.79	8.34
H 4-6	6.67	2.36	13.27	9.24	13.38	8.98
H 7-9	7.45	5.51	12.24	8.40	10.56	8.83
H 10-12	10.98	9.45	6.63	9.66	5.63	8.47
H 13-15	15.29	14.17	1.02	12.61	4.23	9.46
H 16-18	12.55	13.39	7.14	10.50	-0.70	8.58
Average	9.61	6.96	9.61	9.73	7.98	8.78
Optimal	H13/5.48	H16/6.73	H1/13.82	H16/4.79	H1/10.06	H13/ 5.95

Table 8
Percentage reductions in tip deflection of model with chevron braced VE dampers

Model	*El Centro*	*Hachinohe*	*Kobe*	*Northridge*	*S.Fernando*	*Average*
H 1-3	5.49	-0.79	17.35	6.30	12.68	8.21
H 4-6	6.67	6.30	14.80	7.14	9.86	8.95
H 7-9	7.06	9.45	9.18	8.40	5.63	7.95
H 10-12	10.20	12.60	8.16	10.08	2.11	8.63
H 13-15	10.59	14.17	4.08	10.50	0.00	7.87
H 16-18	12.55	13.39	8.67	9.24	-0.70	8.63
Average	8.76	9.19	10.37	8.61	4.93	8.37
Optimal	H16/5.89	H13/6.73	H4/9.09	H7/5.66	H1/7.15	H13/ 5.82

Table 9
Percentage reductions in tip acceleration of model with chevron braced friction dampers

Model	*El Centro*	*Hachinohe*	*Kobe*	*Northridge*	*S.Fernando*	*Average*
H 1-3	1.47	12.22	26.75	-12.10	5.52	6.77
H 4-6	14.89	20.74	25.96	2.23	24.13	17.59
H 7-9	10.80	9.63	3.34	5.77	6.10	7.13
H 10-12	7.86	6.67	2.39	0.56	-0.87	3.32
H 13-15	16.69	5.93	0.80	6.70	2.33	6.49
H 16-18	8.02	-3.70	2.87	-7.82	-12.50	-2.63
Average	9.96	8.58	10.35	-0.78	4.12	6.45
Optimal	H7/13.69	H1/5.77	H16/-0.21	H4/5.63	H7/7.48	H4/ 3.58

Table 10
Percentage reductions in tip acceleration of model with chevron braced VE dampers

Model	*El Centro*	*Hachinohe*	*Kobe*	*Northridge*	*S.Fernando*	*Average*
H 1-3	9.33	9.44	18.79	-7.08	10.76	8.25
H 4-6	18.49	1.85	1.43	5.96	7.56	7.06
H 7-9	11.95	-0.74	-2.39	5.40	0.29	2.90
H 10-12	15.88	3.15	-1.59	-0.37	-8.14	1.78
H 13-15	13.42	-0.74	-1.91	2.98	-9.30	0.89
H 16-18	-3.44	7.78	1.27	-4.66	1.16	0.42
Average	10.94	3.46	2.60	0.37	0.39	3.55
Optimal	H4/10.82	H16/5.77	H16/3.89	H4/11.58	H4/11.97	H4/ 6.02

Table 11
Percentage reductions in tip deflection of model with hybrid friction-VE dampers

Model	*El Centro*	*Hachinohe*	*Kobe*	*Northridge*	*S.Fernando*	*Average*
H 1-3	1.81	-4.68	19.69	6.45	16.70	7.99
H 4-6	7.47	-0.62	10.09	9.81	14.66	8.28
H 7-9	4.64	4.25	12.62	7.29	10.56	7.87
H 10-12	8.27	9.11	5.04	8.55	7.14	7.62
H 13-15	10.70	10.74	2.52	9.39	5.78	7.82
H 16-18	8.68	9.93	9.59	8.97	3.73	8.18
Average	6.93	4.79	9.92	8.41	9.76	7.96
Optimal	H7/9.19	H7/13.04	H10/9.61	H7/11.84	H1/8.37	H7/ 9.45

Table 12
Percentage reductions in tip acceleration of model with hybrid friction-VE dampers

Model	*El Centro*	*Hachinohe*	*Kobe*	*Northridge*	*S.Fernando*	*Average*
H 1-3	10.24	17.02	24.67	-9.37	-1.55	8.20
H 4-6	23.44	17.38	21.42	1.53	17.17	16.19
H 7-9	15.67	6.22	2.39	6.28	-0.13	6.08
H 10-12	16.55	6.76	1.46	2.76	0.43	5.59
H 13-15	20.80	0.82	-3.18	6.98	0.72	5.23
H 16-18	5.11	-0.08	7.19	-3.22	-1.27	1.54
Average	15.30	8.02	8.99	0.82	2.56	7.14
Optimal	H10/47.05	H7/20.03	H7/28.38	H4/6.70	H16/4.97	H7/ 14.09

Table 13
Percentage reductions in tip deflection of model with lower toggle damping systems

Model	*El Centro*	*Hachinohe*	*Kobe*	*Northridge*	*S.Fernando*	*Average*
H 1-3	8.94	-0.18	30.22	9.99	23.74	14.54
H 4-6	4.58	1.41	19.33	17.39	23.07	13.16
H 7-9	8.15	3.80	21.81	13.28	21.06	13.62
H 10-12	10.52	10.16	20.32	13.69	17.05	14.35
H 13-15	13.29	14.93	11.91	17.80	11.03	13.79
H 16-18	15.67	17.31	8.94	17.39	-1.68	11.52
Average	10.19	7.90	18.75	14.92	15.71	13.50
Optimal	H13/7.35	H16/9.84	H1/17.35	H1/9.32	H1/13.79	H13/ 8.77

Table 14
Percentage reductions in tip acceleration of model with lower toggle damping systems

Model	*El Centro*	*Hachinohe*	*Kobe*	*Northridge*	*S.Fernando*	*Average*
H 1-3	10.19	-2.01	25.73	30.39	40.52	20.96
H 4-6	33.47	25.55	24.83	32.46	18.84	27.03
H 7-9	21.97	12.66	19.22	11.10	-0.89	12.81
H 10-12	18.66	4.97	9.67	5.24	9.67	9.64
H 13-15	35.91	30.56	29.07	15.23	16.06	25.37
H 16-18	6.88	-2.01	3.00	-26.98	-13.40	-6.50
Average	21.18	11.62	18.59	11.24	11.80	14.89
Optimal	H13/29.33	H1/7.75	H1/10.47	H7/12.26	H7/13.75	H4/ 11.39

Table 15
Reductions in tip deflection and acceleration of model with combined damping system

	El Centro	Hachinohe	Kobe	Northridge	S.Fernando	Average
% Defl. Red.	26.16	19.18	7.36	25.31	6.92	16.99
% Accel. Red.	15.55	25.85	14.80	13.28	8.82	15.66

Table16
Tip deflection and tip acceleration of the undamped 12-storey structure.

	El Centro	*Hachinohe*	*Kobe*	*Northridge*	*S.Fernando*
Deflection(m)	0.206	0.374	0.154	0.145	0.141
Acceleration(m/s^2)	5.69	6.61	6.93	5.76	3.51

Table 17
Percentage reductions in tip deflection of model with diagonal friction dampers

Model	*El Centro*	*Hachinohe*	*Kobe*	*Northridge*	*S.Fernando*	*Average*
M 1-2	28.99	4.46	-8.44	-2.07	0.68	4.72
M 3-4	19.32	9.82	1.30	10.34	8.16	9.79
M 5-6	18.36	3.57	20.13	17.93	14.97	14.99
M 7-8	35.75	4.46	13.64	24.14	21.09	19.82
M 9-10	30.92	9.82	-1.95	28.97	23.13	18.18
M 11-12	33.82	9.82	8.44	28.97	22.45	20.70
Average	27.86	6.99	5.52	18.05	15.08	14.70
Optimal	M11/23.87	M3/6.20	M7/20.41	M9/16.18	M11/14.52	M11/14.46

Table 18
Floors with largest interstorey drift

Drift	*El Centro*	*Hachinohe*	*Kobe*	*Northridge*	*S.Fernando*
1st largest	9-10	9-10	10-11	6-7	10-11
2nd largest	10-11	10-11	9-10	7-8	9-10
3rd largest	8-9	8-9	8-9	8-9	8-9

Table 19
Percentage reductions in tip deflection of model with diagonal VE dampers

Model	*El Centro*	*Hachinohe*	*Kobe*	*Northridge*	*S.Fernando*	*Average*
M 1-2	39.61	5.36	25.32	-5.52	6.80	14.32
M 3-4	41.06	5.36	15.58	-0.69	10.88	14.44
M 5-6	42.03	6.25	12.34	3.45	9.52	14.72
M 7-8	39.13	8.93	18.83	2.07	8.84	15.56
M 9-10	14.98	2.68	18.18	2.76	3.40	8.40
M 11-12	0.48	-4.46	14.29	2.76	1.36	2.88
Average	29.55	4.02	17.42	0.80	6.80	11.72
Optimal	M3/30.92	M5/5.36	M11/14.29	M7/6.21	M72.72	M7/7.87

Table 20
Percentage reductions in tip acceleration of model with diagonal friction dampers

Model	*El Centro*	*Hachinohe*	*Kobe*	*Northridge*	*S.Fernando*	*Average*
M 1-2	27.24	23.87	8.65	9.53	-9.38	11.98
M 3-4	22.67	11.63	19.74	14.38	-2.27	13.23
M 5-6	15.99	-9.82	20.89	2.95	2.84	6.57
M 7-8	26.19	-4.68	-10.23	15.94	-8.24	3.80
M 9-10	13.18	-3.78	4.61	22.18	-21.31	2.98
M 11-12	-8.44	-11.33	-1.15	-1.91	-17.33	-8.03
Average	16.14	0.98	7.08	10.51	-9.28	5.09
Optimal	M1/27.41	M9/6.49	M11/23.27	M11/17.53	M3/-4.76	M7/5.18

Table 21
Percentage reductions in tip acceleration of model with diagonal VE dampers

Model	*El Centro*	*Hachinohe*	*Kobe*	*Northridge*	*S.Fernando*	*Average*
M 1-2	42.88	25.98	12.25	-3.64	8.24	17.14
M 3-4	28.82	18.13	19.74	0.69	13.92	16.26
M 5-6	16.17	8.46	4.18	0.35	18.75	9.58
M 7-8	12.83	6.34	5.33	-1.21	7.10	6.08
M 9-10	11.60	6.04	21.18	-2.43	1.70	7.62
M 11-12	-3.69	-0.76	17.29	-10.23	-10.80	-1.64
Average	18.10	10.70	13.33	-2.74	6.49	9.17
Optimal	M1/14.41	M3/6.95	M11/9.22	M5/2.60	M3/9.66	M3/5.25

Table 22
Percentage reductions in tip deflection of model with chevron brace friction dampers

Model	*El Centro*	*Hachinohe*	*Kobe*	*Northridge*	*S.Fernando*	*Average*
M 1-2	0.48	1.79	18.18	6.90	4.08	6.29
M 3-4	5.31	3.57	18.83	11.03	12.24	10.20
M 5-6	24.15	2.68	15.58	15.17	13.61	14.24
M 7-8	32.85	3.57	16.23	18.62	18.37	17.93
M 9-10	33.33	2.68	11.04	20.00	20.41	17.49
M 11-12	32.85	1.79	15.58	17.24	17.01	16.89
Average	21.50	2.68	15.91	14.83	14.29	13.84
Optimal	M9/27.35	M3/0.68	M1/16.40	M9/14.05	M9/18.02	M9/14.26

Table 23
Percentage reductions in tip deflection of model with chevron brace VE dampers

Model	*El Centro*	*Hachinohe*	*Kobe*	*Northridge*	*S.Fernando*	*Average*
M 1-2	-0.97	1.79	18.18	6.90	4.76	6.13
M 3-4	6.76	2.68	19.48	8.97	7.48	9.07
M 5-6	8.70	2.68	16.88	11.72	10.88	10.17
M 7-8	16.43	3.57	19.48	13.79	11.56	12.97
M 9-10	22.22	1.79	20.13	14.48	11.56	14.04
M 11-12	27.05	0.89	14.94	15.17	13.61	14.33
Average	13.37	2.23	18.18	11.84	9.98	11.12
Optimal	M11/16.41	M3/0.68	M3/16.40	M11/11.21	M119.61	M11/9.82

Table 24
Percentage reductions in tip acceleration of model with chevron brace friction dampers

Model	*El Centro*	*Hachinohe*	*Kobe*	*Northridge*	*S.Fernando*	*Average*
M 1-2	-14.41	-16.47	-8.79	-23.57	-20.17	-16.68
M 3-4	-12.30	-7.25	19.45	-8.15	-49.72	-11.59
M 5-6	-9.84	0.15	17.00	10.75	-49.15	-6.22
M 7-8	-22.50	-9.06	12.54	-1.04	-66.19	-17.25
M 9-10	-27.94	-4.08	0.00	3.29	-52.84	-16.31
M 11-12	-44.82	-24.92	14.84	-17.33	-89.49	-32.34
Average	-21.97	-10.27	9.17	-6.01	-54.59	-16.73
Optimal	M3/-8.07	M3/-2.22	M9/25.64	M3/2.36	M3/-18.22	M3/-2.77

Table 25
Percentage reductions in tip acceleration of model with chevron brace VE dampers

Model	*El Centro*	*Hachinohe*	*Kobe*	*Northridge*	*S.Fernando*	*Average*
M 1-2	-6.50	-9.52	2.31	-15.77	-13.35	-8.57
M 3-4	-2.64	-6.95	11.38	-9.71	-8.24	-3.23
M 5-6	-8.44	-1.81	13.54	11.79	-21.59	-1.30
M 7-8	4.39	-6.50	14.70	1.91	-43.75	-5.85
M 9-10	-28.65	-4.53	20.03	4.16	-54.55	-12.71
M 11-12	-42.88	-20.24	25.36	-17.33	-78.13	-26.64
Average	-14.12	-8.26	14.55	-4.16	-36.60	-9.72
Optimal	M3/-2.64	M5/2.91	M3/22.08	M5/-6.03	M3/-7.68	M3/0.02

Table 26
Percentage reductions in tip deflection of model with hybrid friction-VE dampers

Model	*El Centro*	*Hachinohe*	*Kobe*	*Northridge*	*S.Fernando*	*Average*
M 1-2	30.60	6.17	24.74	-0.72	1.82	12.52
M 3-4	27.03	11.33	14.32	3.58	0.18	11.29
M 5-6	23.96	12.19	9.68	7.89	7.55	12.25
M 7-8	14.27	9.61	6.79	7.89	9.18	9.55
M 9-10	10.19	7.89	7.95	9.61	11.64	9.45
M 11-12	4.06	9.61	12.00	10.47	14.09	10.05
Average	18.35	9.47	12.58	6.45	7.41	10.85
Optimal	M1/20.89	M3/8.64	M1/8.44	M7/8.64	M118.92	M3/7.54

Table 27
Percentage reductions in tip acceleration of model with hybrid friction-VE dampers

Model	*El Centro*	*Hachinohe*	*Kobe*	*Northridge*	*S.Fernando*	*Average*
M 1-2	22.87	20.78	1.24	8.07	-3.59	9.87
M 3-4	-2.89	29.79	19.20	11.03	4.44	12.31
M 5-6	-3.64	25.61	14.83	10.21	-1.68	9.07
M 7-8	-4.84	9.90	6.34	12.51	0.43	4.87
M 9-10	3.70	19.57	10.95	13.99	4.82	10.61
M 11-12	-4.09	12.10	6.70	4.95	-12.95	1.34
Average	1.85	19.62	9.88	10.13	-1.42	8.01
Optimal	M9/-0.04	M9/27.41	M11/7.86	M9/7.78	M11/0.78	M9/6.77

Table 28
Percentage reductions in tip deflection of model with lower toggle VE dampers

Model	*El Centro*	*Hachinohe*	*Kobe*	*Northridge*	*S.Fernando*	*Average*
M 1-2	26.50	9.75	28.53	4.69	3.80	14.65
M 3-4	35.00	12.28	30.23	6.37	8.61	18.50
M 5-6	30.50	15.65	18.32	12.28	7.81	16.91
M 7-8	21.00	14.81	11.51	13.12	16.63	15.41
M 9-10	10.50	13.97	14.35	15.65	23.04	15.50
M 11-12	7.50	16.50	9.24	19.03	22.24	14.90
Average	21.83	13.82	18.69	11.86	13.69	15.98
Optimal	M1/23.71	M1/12.17	M1/9.94	M11/9.57	M11/12.40	M5/10.71

Table 29
Percentage reductions in tip acceleration of model with lower toggle VE dampers

Model	*El Centro*	*Hachinohe*	*Kobe*	*Northridge*	*S.Fernando*	*Average*
M 1-2	4.61	19.90	29.39	1.71	-6.36	9.85
M 3-4	30.74	26.47	14.53	16.53	8.43	19.34
M 5-6	12.83	33.36	26.89	19.11	-6.55	17.13
M 7-8	6.38	33.68	23.68	16.37	3.19	16.66
M 9-10	14.45	26.90	20.71	24.91	18.17	21.03
M 11-12	-39.12	-9.60	-10.19	4.77	-37.45	-18.32
Average	4.98	21.79	17.50	13.90	-3.43	10.95
Optimal	M9/2.72	M9/31.30	M5/9.80	M9/12.46	M3/7.92	M9/11.35

Table 30
Reduction tip deflection and tip acceleration of the model with combined damping system

	El Centro	Hachinohe	Kobe	Northridge	S.Fernando	Average
% Defl. Red.	26.70	12.30	27.26	20.69	17.73	20.93
% Accel. Red.	26.53	15.13	33.47	9.02	11.36	19.10